Dose calculation methods

Mike Stabin
Vanderbilt University, USA

MetroMRT 3rd Workshop
"Clinical implementation of dosimetry for molecular radiotherapy"
National Physical Laboratory, Teddington, UK
20-21 April 2015

MIRD

$$D(r_T, T_D) = \int_0^{T_D} \dot{D}(r_T, t)dt$$

$$= \sum_{r_S} \int_0^{T_D} A(r_S, t) S(r_T \leftarrow r_S, t)dt,$$

$$S(r_T \leftarrow r_S, t) = \frac{1}{M(r_T, t)} \sum_i E_i Y_i \phi(r_T \leftarrow r_S, E_i, t)$$

ICRP

$$\boldsymbol{H_{50,T} = \sum_S U_S \, SEE(T \leftarrow S)}$$

$$SEE = \frac{k \sum_i n_i E_i \phi_i Q_i}{m}$$

RADAR method (Health Phys 85(3):294-310, 2003):

$$D = N \times DCF$$

N is the number of disintegrations that occur in a source region

DCF is the dose conversion factor, which gives the dose absorbed in a target per disintegration in a source

Concepts

- Internal dose estimates – “marriage” of physical and biological quantities
- Biology – distribution and kinetics
- Physics – energy deposition patterns

$$D = \left(\tilde{A} / A_0 \right) DF$$

$$D = \begin{bmatrix} (\tilde{A}/A_0)_{kid} & (\tilde{A}/A_0)_{blad1} & (\tilde{A}/A_0)_{RB} \\ (\tilde{A}/A_0)_{kid} & (\tilde{A}/A_0)_{blad2} & (\tilde{A}/A_0)_{RB} \end{bmatrix} X$$

$$\begin{bmatrix} DF(kid \leftarrow kid) & DF(ov \leftarrow kid) & DF(mar \leftarrow kid) & DF(test \leftarrow kid) & DF(blad \leftarrow kid) & DF(TB \leftarrow kid) \\ DF(kid \leftarrow blad) & DF(ov \leftarrow blad) & DF(mar \leftarrow blad) & DF(test \leftarrow blad) & DF(blad \leftarrow blad) & DF(RB \leftarrow blad) \\ DF(kid \leftarrow RB) & DF(ov \leftarrow RB) & DF(mar \leftarrow RB) & DF(test \leftarrow RB) & DF(blad \leftarrow RB) & DF(TB \leftarrow RB) \end{bmatrix}$$

$$D = \begin{bmatrix} 0.092 & 0.842 & 2.84 \\ 0.092 & 1.72 & 2.84 \end{bmatrix} \begin{bmatrix} 1.32x10^{-5} & 7.02x10^{-8} & 1.71x10^{-7} & 3.10x10^{-9} & 1.87x10^{-8} & 1.58x10^{-7} \\ 2.00x10^{-8} & 5.41x10^{-7} & 8.02x10^{-8} & 3.73x10^{-7} & 1.10x10^{-5} & 1.18x10^{-7} \\ 1.54x10^{-7} & 1.81x10^{-7} & 1.34x10^{-7} & 1.28x10^{-7} & 1.67x10^{-7} & 1.39x10^{-7} \end{bmatrix}$$

$$D = \begin{bmatrix} D_{kid_1} & D_{ov_1} & D_{mar_1} & D_{test_1} & D_{blad_1} & D_{TB_1} \\ D_{kid_2} & D_{ov_2} & D_{mar_2} & D_{test_2} & D_{blad_2} & D_{TB_2} \end{bmatrix}$$

$$D = \begin{bmatrix} 5.5x10^{-3} & 3.5x10^{-3} & 1.7x10^{-3} & 2.4x10^{-3} & 3.5x10^{-2} & 1.8x10^{-3} \\ 5.5x10^{-3} & 5.2x10^{-3} & 1.9x10^{-3} & 3.6x10^{-3} & 7.0x10^{-2} & 2.2x10^{-3} \end{bmatrix}$$

(units are mGy / MBq)

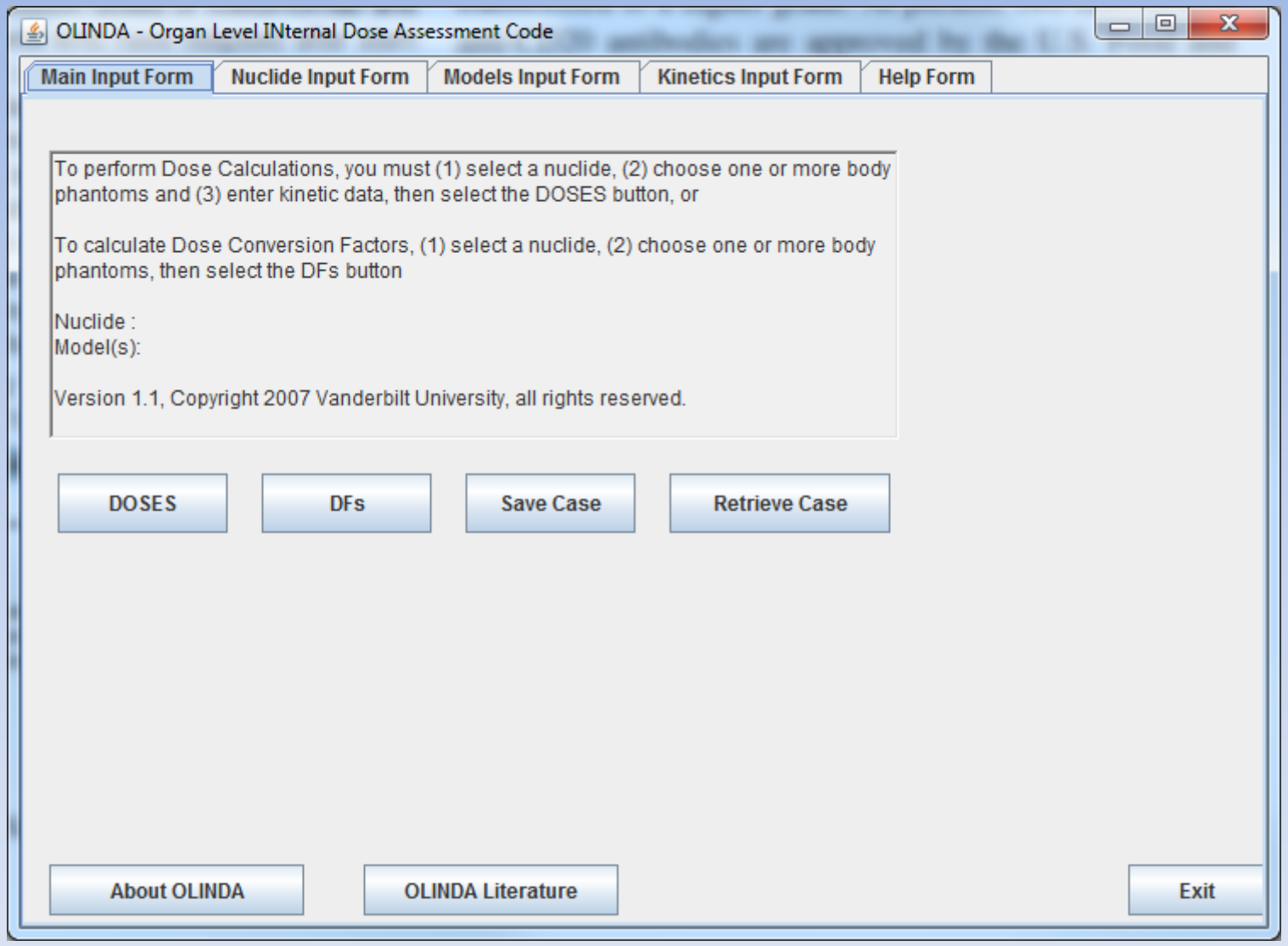
OLINDA - Organ Level INternal Dose Assessment Code
Main Input Form
Nuclide Input Form
Models Input Form
Kinetics Input Form
Help Form
To perform Dose Calculations, you must (1) select a nuclide, (2) choose one or more body phantoms and (3) enter kinetic data, then select the DOSES button, or
To calculate Dose Conversion Factors, (1) select a nuclide, (2) choose one or more body phantoms, then select the DFs button
Nuclide :
Model(s):
Version 1.1, Copyright 2007 Vanderbilt University, all rights reserved.
DOSES
DFs
Save Case
Retrieve Case
About OLINDA
OLINDA Literature
Exit

Radiation Dose Estimates (mSv/MBq) for F-18 FDG

Biokinetic data: ICRP 106 recommended model

Physical models: RADAR ICRP 89 Reference Phantom Series

Effective doses: ICRP 103 weighting factors

	Males				
	Adult	15-yo	10-yo	5-yo	1-yo
Adrenals	1.35E-02	1.73E-02	2.57E-02	4.07E-02	7.06E-02
Brain	3.56E-02	3.65E-02	3.79E-02	4.21E-02	5.79E-02
Breasts	7.01E-03	8.95E-03	- - -	- - -	- - -
Esophagus	1.28E-02	1.63E-02	2.61E-02	4.21E-02	7.73E-02
Eyes	1.03E-02	1.26E-02	1.88E-02	2.94E-02	5.14E-02
Gallbladder Wall	1.42E-02	1.70E-02	2.56E-02	3.77E-02	6.46E-02
Left colon	1.15E-02	1.35E-02	2.23E-02	3.44E-02	6.01E-02
Small Intestine	1.24E-02	1.55E-02	2.49E-02	3.89E-02	6.78E-02
Stomach Wall	1.25E-02	1.55E-02	2.37E-02	3.71E-02	6.44E-02
Right colon	1.18E-02	1.45E-02	2.26E-02	3.55E-02	6.16E-02
Rectum	1.58E-02	1.90E-02	3.26E-02	4.80E-02	7.42E-02
Heart Wall	6.35E-02	8.73E-02	1.40E-01	2.24E-01	3.79E-01
Kidneys	2.05E-02	2.53E-02	3.49E-02	5.54E-02	8.76E-02
Liver	2.21E-02	2.92E-02	4.28E-02	6.19E-02	1.03E-01
Lungs	1.76E-02	2.29E-02	3.74E-02	5.92E-02	1.12E-01
Pancreas	1.28E-02	1.62E-02	2.52E-02	3.94E-02	7.12E-02
Prostate	1.83E-02	2.21E-02	5.51E-02	4.97E-02	6.97E-02
Salivary Glands	1.14E-02	1.42E-02	2.17E-02	3.35E-02	5.88E-02
Red Marrow	9.75E-03	1.47E-02	2.23E-02	3.08E-02	5.48E-02
Osteogenic Cells	1.53E-02	2.07E-02	3.17E-02	4.51E-02	8.58E-02
Spleen	1.05E-02	1.34E-02	2.07E-02	3.39E-02	6.03E-02
Testes	1.02E-02	1.29E-02	2.44E-02	3.11E-02	5.54E-02
Thymus	1.33E-02	1.72E-02	2.48E-02	4.01E-02	7.07E-02
Thyroid	1.01E-02	1.29E-02	2.08E-02	3.39E-02	6.18E-02
Urinary Bladder Wall	1.36E-01	1.69E-01	2.55E-01	3.47E-01	4.62E-01
Effective Doses	1.73E-02	2.21E-02	3.26E-02	4.76E-02	7.83E-02

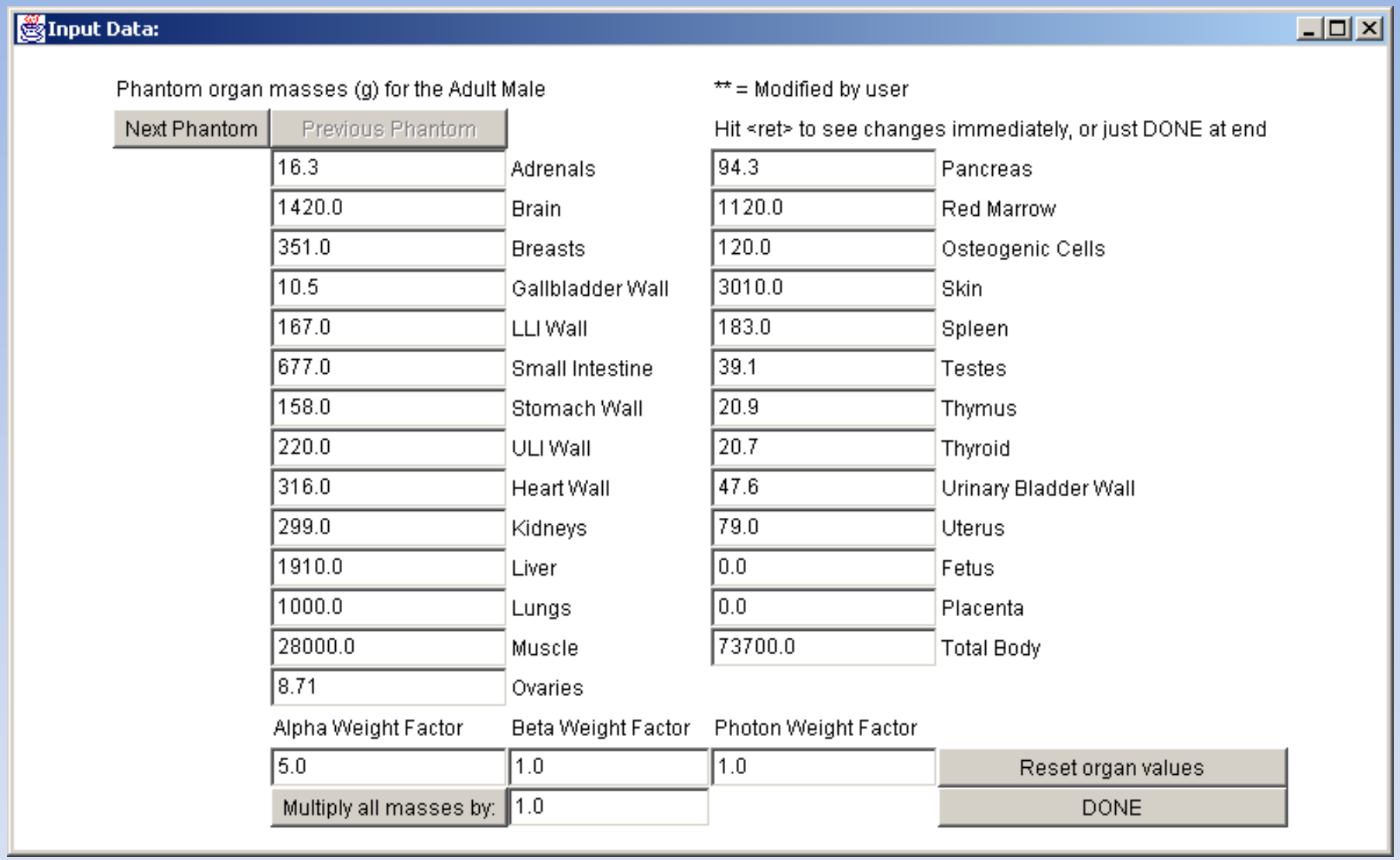
Input Data:
Phantom organ masses (g) for the Adult Male
** = Modified by user
Next Phantom
Previous Phantom
Hit <ret> to see changes immediately, or just DONE at end
16.3
Adrenals
94.3
Pancreas
1420.0
Brain
1120.0
Red Marrow
351.0
Breasts
120.0
Osteogenic Cells
10.5
Gallbladder Wall
3010.0
Skin
167.0
LLI Wall
183.0
Spleen
677.0
Small Intestine
39.1
Testes
158.0
Stomach Wall
20.9
Thymus
220.0
ULI Wall
20.7
Thyroid
316.0
Heart Wall
47.6
Urinary Bladder Wall
299.0
Kidneys
79.0
Uterus
1910.0
Liver
0.0
Fetus
1000.0
Lungs
0.0
Placenta
28000.0
Muscle
73700.0
Total Body
8.71
Ovaries
Alpha Weight Factor
Beta Weight Factor
Photon Weight Factor
5.0
1.0
1.0
Reset organ values
Multiply all masses by:
1.0
DONE

Organ Mass Scaling

- For electrons, the scaling is:

$$DF_2 = DF_1 \frac{m_1}{m_2}$$

- For photons, the scaling is:

$$\phi_2 = \phi_1 \left(\frac{m_2}{m_1} \right)^{1/3} \qquad \Phi_2 = \Phi_1 \left(\frac{m_1}{m_2} \right)^{2/3}$$

Patient-Individualized Medicine

The Case for Patient-Specific Dosimetry in Radionuclide Therapy

CANCER BIOTHERAPY & RADIOPHARMACEUTICALS
Volume 23, Number 3, 2008

- "Treating all nuclear medicine patients with a single, uniform method of activity administration amounts to consciously choosing that these patients be treated with a lower standard of care than patients who receive radiation externally for cancer treatments."

Dosimetry

- Administration of 500 MBq of I-131
- Thyroid uptake 55% at 24 hours
- Uptake half-time 6 hours, elimination half-time 7 days:

$$A_{thy} = 500\ MBq\left(\frac{10^6\ dis}{MBq - s}\right)\times 0.55\times\left(\exp^{\frac{-0.693\times 24h}{168h}} - \exp^{\frac{-0.693\times 24h}{6\,h}}\right)$$

$$N_{thy} = 2.75x10^8\ \frac{dis}{\sec}\left(\frac{1}{0.004125\,h^{-1}} - \frac{1}{0.1125\,h^{-1}}\right)\left(\frac{3600\ s}{h}\right) = 2.31x10^{14}\ dis$$

Dosimetry

$$D = \left(\frac{2.31\,x\,10^{14}\ dis}{\text{sec}}\right)\left(\frac{0.192\ MeV}{\beta}\right)\left(\frac{0.899\ \beta}{dis}\right)\left(\frac{1.602\,x\,10^{-13}\ Joule}{MeV}\right)\left(\frac{kg\text{-}Gy}{1\ J}\right)\left(\frac{1}{0.020\ kg}\right)$$

$$D = 320\ Gy$$

- Contributions from other electrons and photons, estimate becomes ~430 Gy.

Patient-Specific Modifications

- Traino, DiMartino et al. – adjustment for change in thyroid mass during dose delivery

$$D_T = \frac{\sigma A_m T}{2m_0} + \frac{\sigma}{k}\left[m_0 - \left(m_0^2 - \frac{2kA_m}{c} \right)^{1/2} \right]$$

Patient-Individualized Medicine

- Using a fixed activity or activity/body size gives very different therapeutic benefit to different patients.
- Individual kinetics and body morphologies are highly variable.

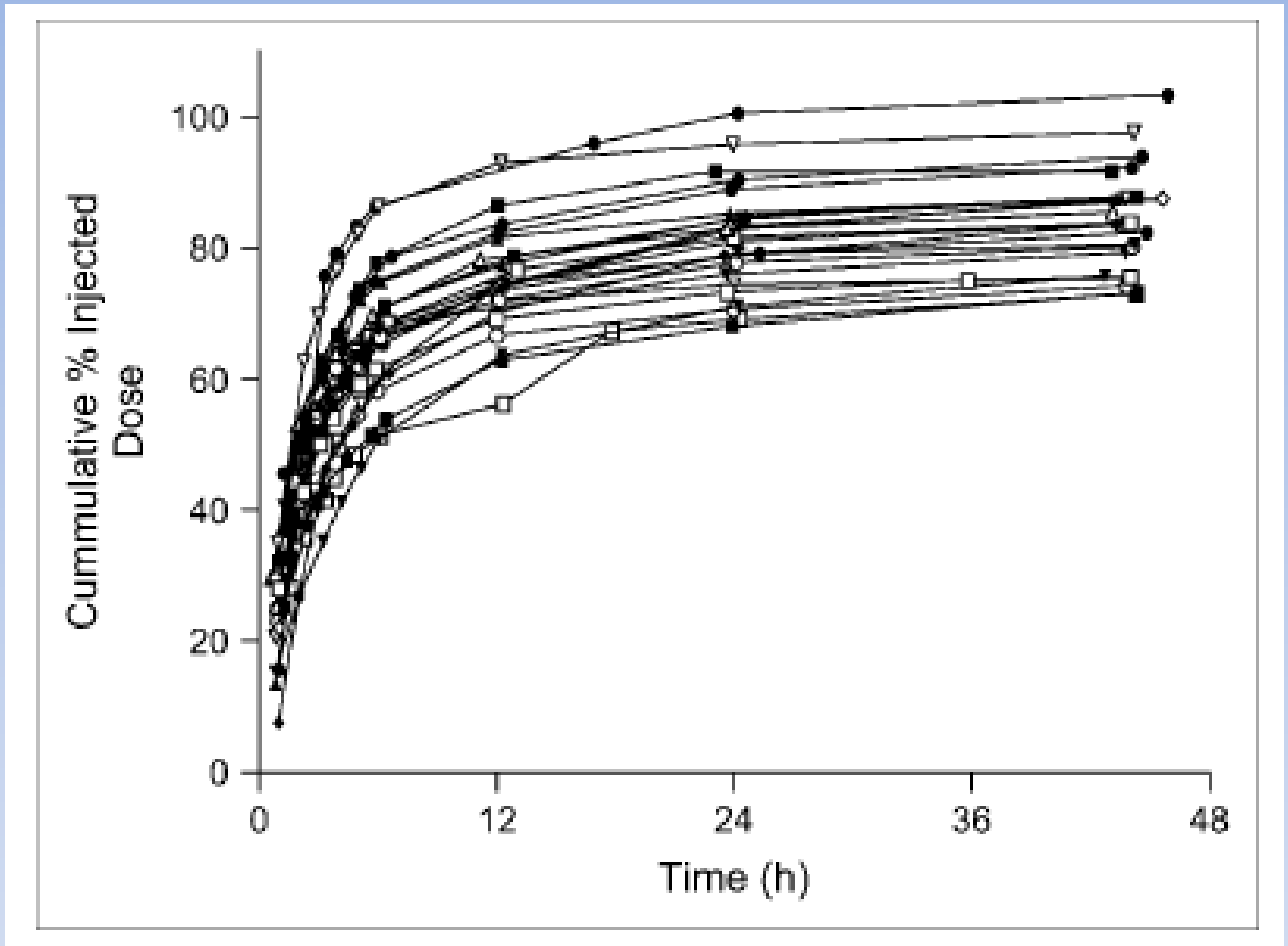

Cumulative excretion of Ho-166 DOTMP in twelve subjects (6 ♀, 6 ♂) with multiple myeloma. Breitz et al. J Nucl Med 2006

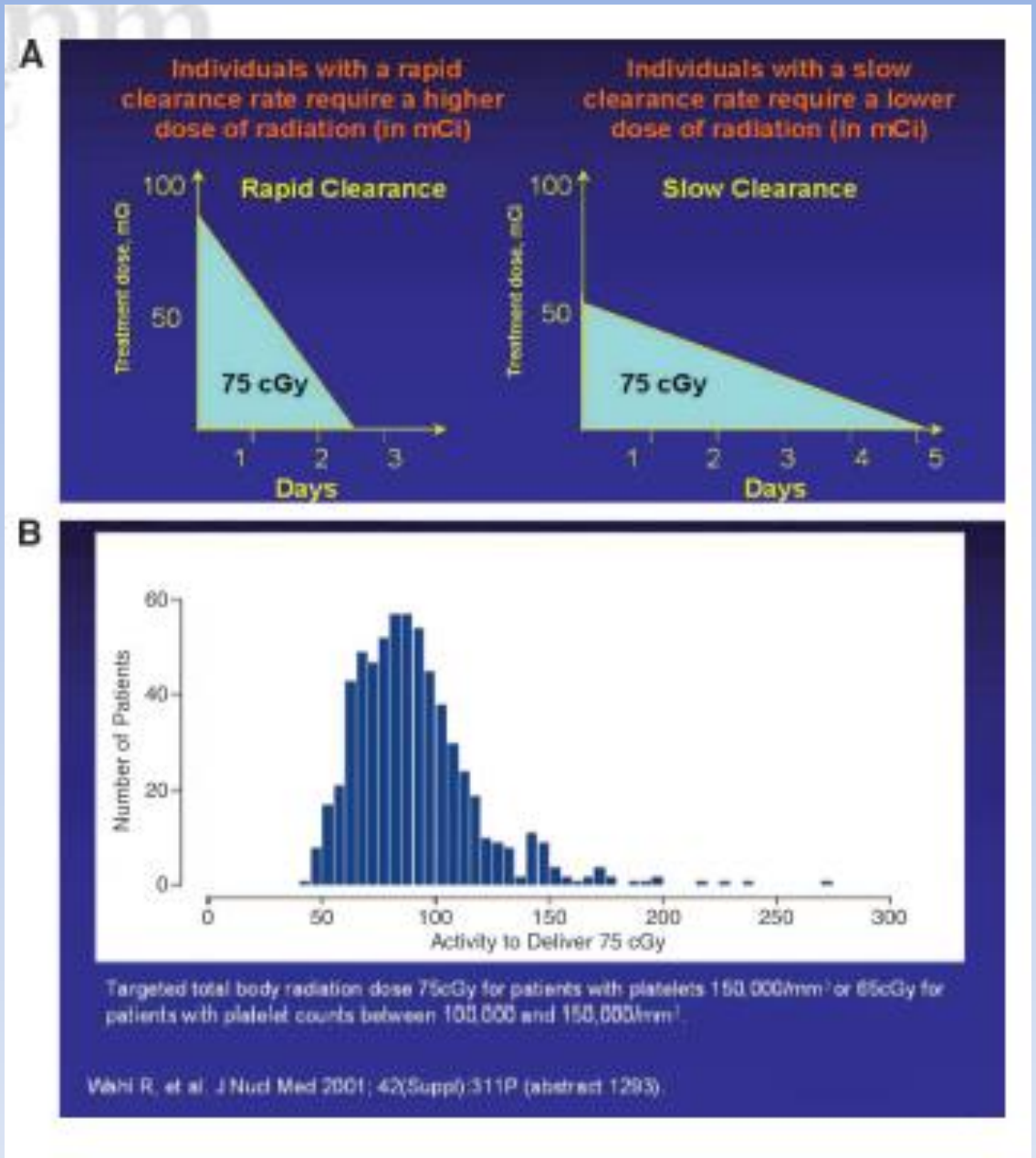

Wahl, J Nucl Med 2005; 46:128S–140S

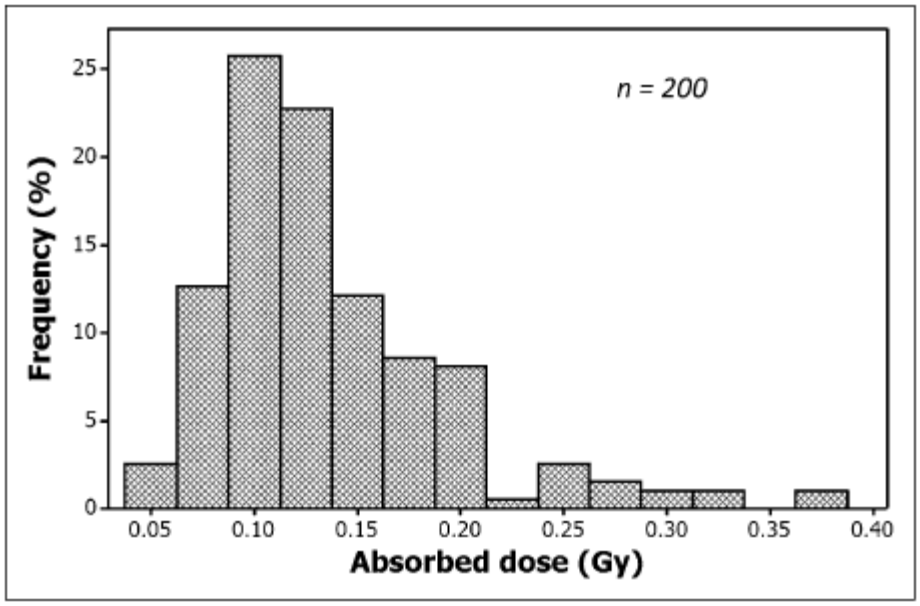

FIGURE 3. Total absorbed dose to bone marrow of 200 patients for a single therapy cycle.

Sandstrom et al. JNM 2013:54:33-41

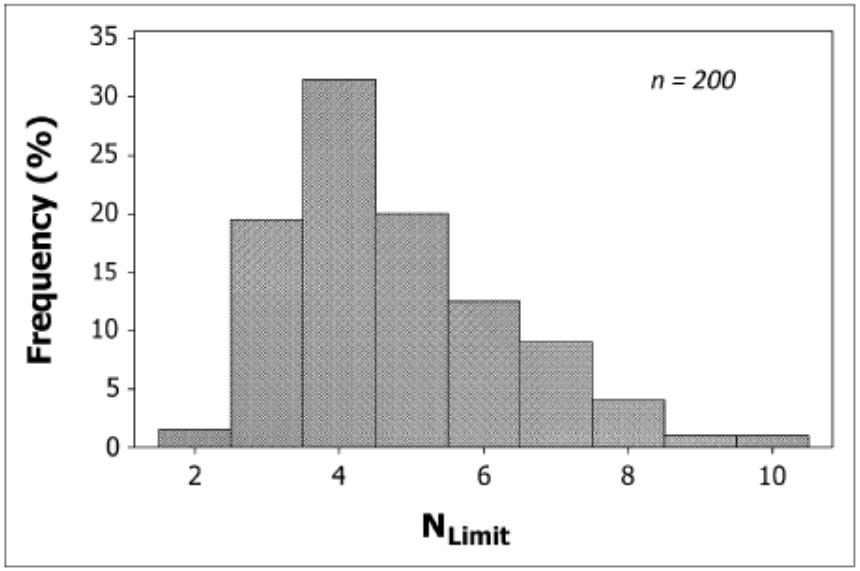

FIGURE 7. Maximum tolerable number of cycles with respect to absorbed doses to bone marrow and kidneys for 200 patients.

TABLE 2

Recent Physical Phantom Evaluations of SPECT Quantification of Radionuclides Relevant to Internal Radionuclide Therapy as Well as ^{99m}Tc

Study	Radionuclide	System	Reconstruction	Absolute quantification accuracy
Zeintl et al., 2010 (*18*)	^{99m}Tc	SPECT/CT	OS-EM, CDR, CT-derived AC, energy window–based SC, PVC	<6.8% error for 0.5- to 16-mL spheres
Dewaraja et al., 2010 (*37*)	^{131}I	SPECT/CT	OS-EM, CDR, CT-derived AC, energy window–based SC	<17% error for 8- to 95-mL spheres; 31% for 4-mL sphere
Assie et al., 2010 (*23*)	^{111}In	SPECT and CT separate	OS-EM, CT-derived AC, energy window–based SC, PVC	<20% error for organs and 2- to 32-mL spheres; 48% error for 0.5-mL sphere
Shcherbinin et al., 2008 (*49*)	^{99m}Tc, ^{111}In, ^{123}I, ^{131}I	SPECT/CT	OS-EM, CDR, CT-derived AC, analytic scatter modeling	3%–5% error for 32-mL bottles
Minarik et al., 2008 (*95*)	^{90}Y	SPECT/CT	OS-EM, CDR, CT-derived AC, ESSE	<11% error for liver and 100-mL sphere
Willowson et al., 2008 (*19*)	^{99m}Tc	SPECT/CT	OS-EM, CT-derived AC, transmission-dependent SC, PVC	<4% error for liver and cardiac chambers
de Wit et al., 2006 (*59*)	^{166}Ho	SPECT	OS-EM, CDR, ^{153}Gd transmission source–derived AC, Monte Carlo scatter modeling	16% average error for 220-mL bottles
Du et al., 2006 (*62*)	^{123}I	SPECT/CT	OS-EM, CDR, CT-derived AC, ESSE, PVC	<2% error for putamen and caudate regions of brain phantom
He at al, 2005 (*52*)	^{111}In	SPECT/CT	OS-EM, CDR, CT-derived AC, ESSE, PVC	<12% error for organs and 8- to 23-mL spheres
Koral et al., 2005 (*50*)	^{131}I	SPECT and CT separate	OS-EM, CDR, CT-derived AC, energy window–based SC, PVC	<7% average error for 100-mL sphere

AC = attenuation correction; SC = scatter correction.

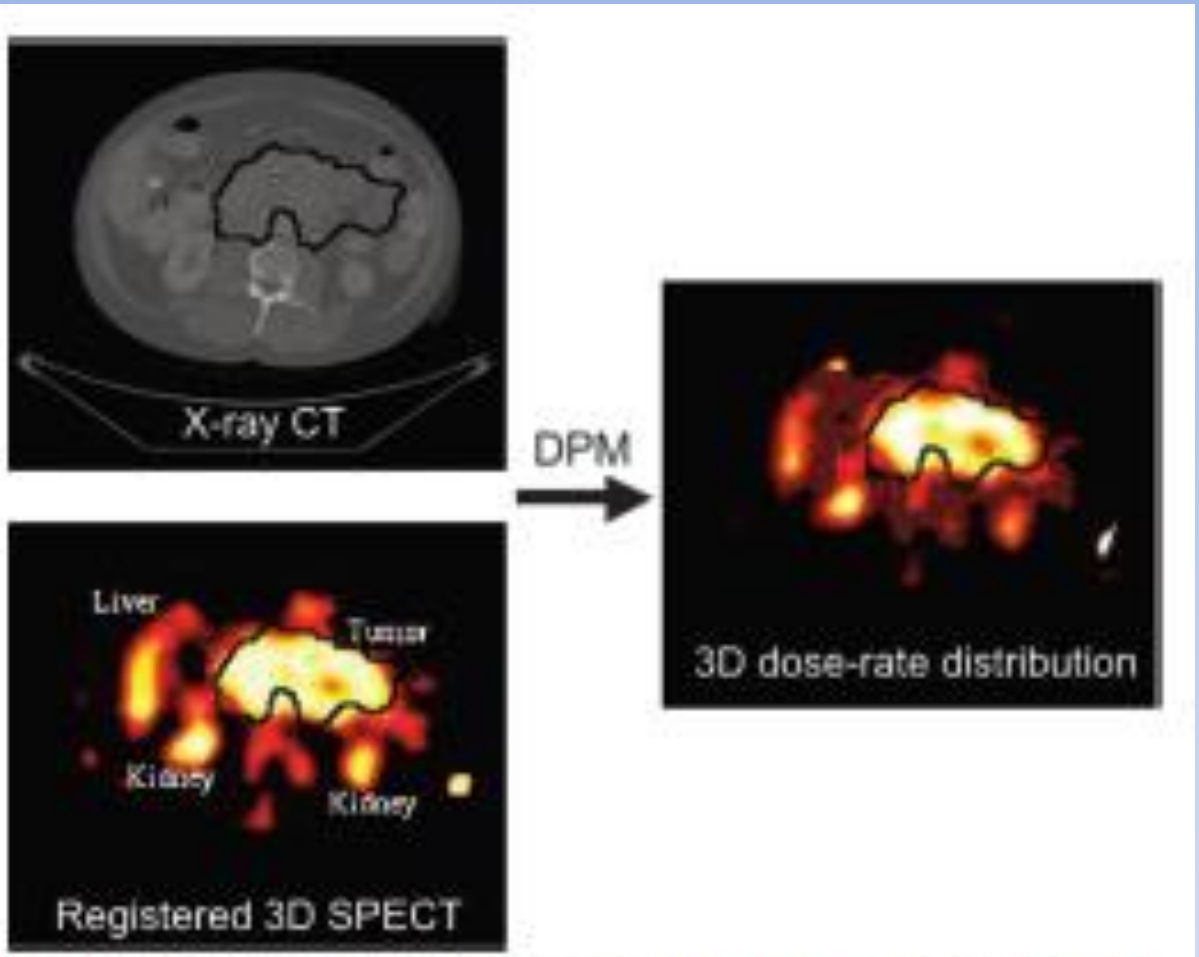

FIGURE 4. One slice of RIT patient CT image, SPECT image, and corresponding dose-rate map.

Dewaraja et al. J Nucl Med 2005; 46:840–849

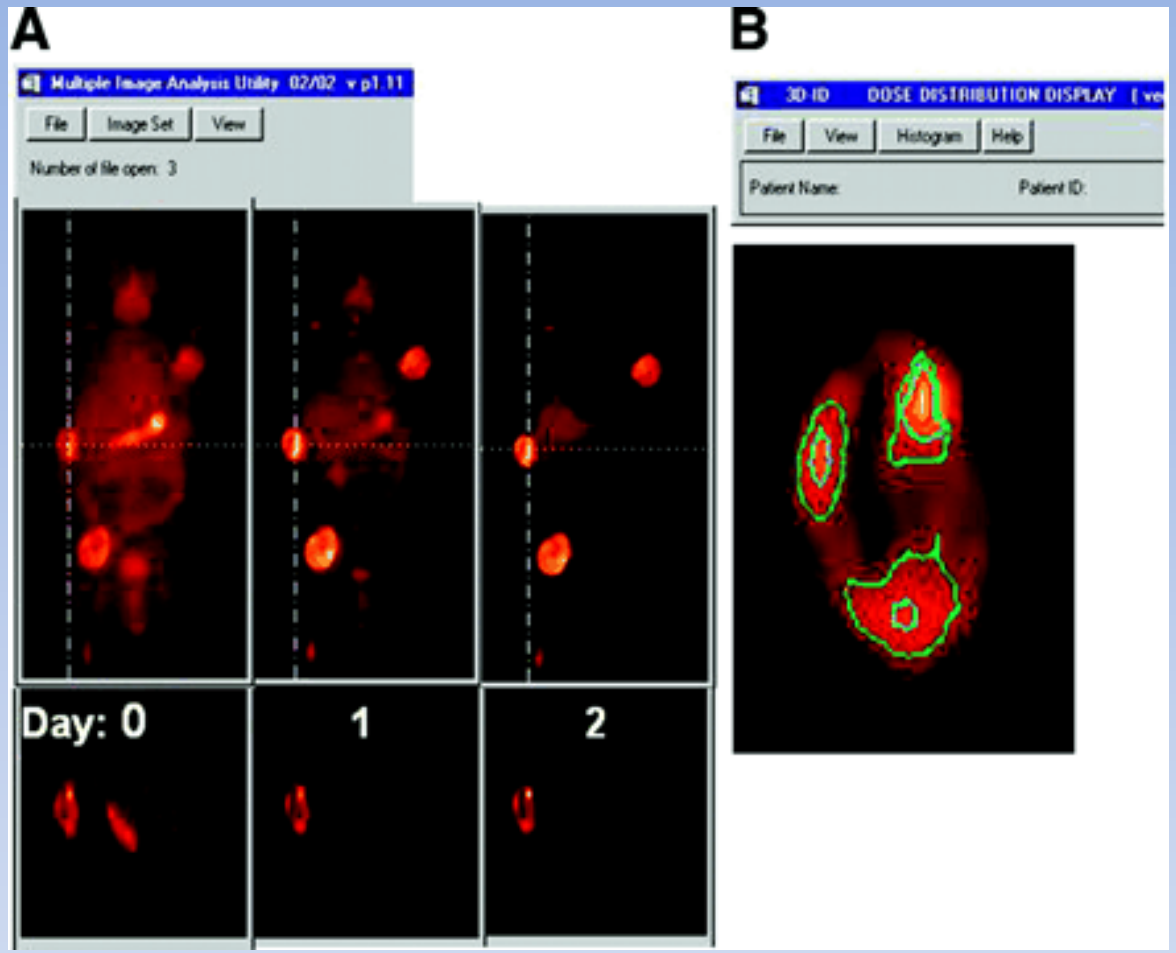

FIGURE 3. (A) Summed coronal ^{124}I PET image slices obtained on day of ^{124}I administration (day 0) and on subsequent 2 days are depicted using same intensity level. Cross-hairs show plane of intersection for corresponding transverse slices through tumor 2, shown immediately below coronal images. (B) Image of absorbed dose distribution in tumor 2, magnified to highlight spatial distribution of absorbed dose within this tumor. Color-coded isodose contours are superimposed as follows: yellow = 75%, red = 50%, blue = 25%, and green = 10% of maximum absorbed dose to tumor (400 Gy). Three different foci of enhanced absorbed dose are observed and designated 1–3 as shown. Kolbert et al. J Nucl Med Vol. 45 No. 8 1366-1372.

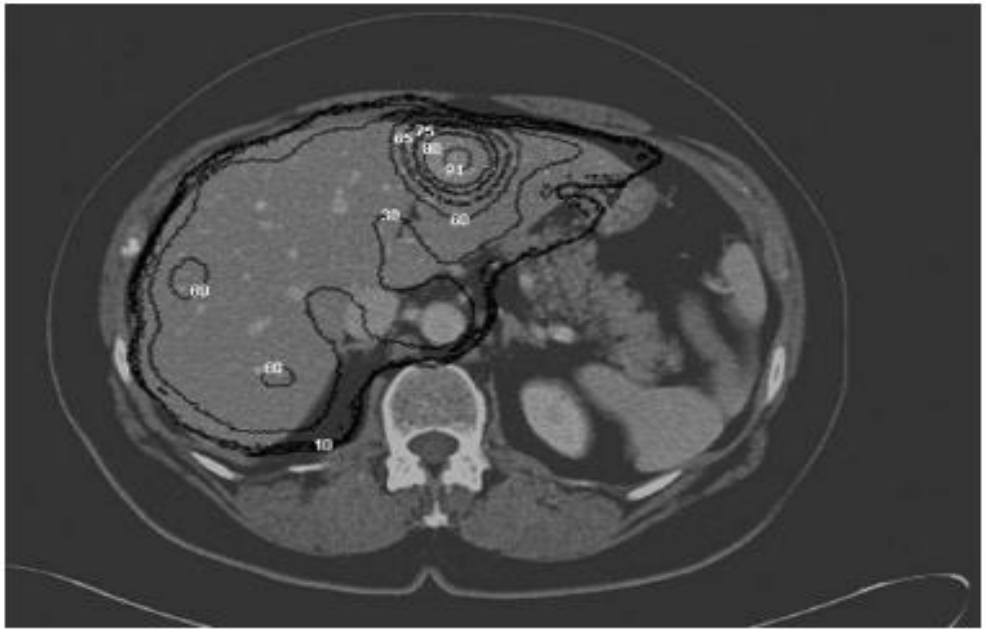

FIG. 7. Calculated dose distribution after administration of ^{131}I-MIBG superimposed on axial CT scan.

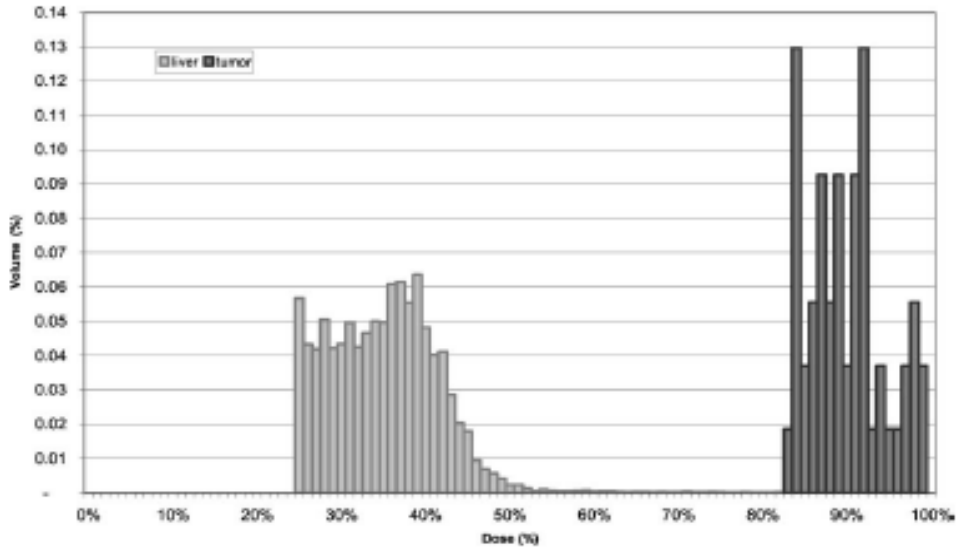

FIG. 8. Differential dose volume histogram for normal liver and metastasis of the case presented in this study.

Strigari *et al.*: Tumor control probability in systemic radiotherapy Medical Physics, Vol. 33, No. 6, June 2006

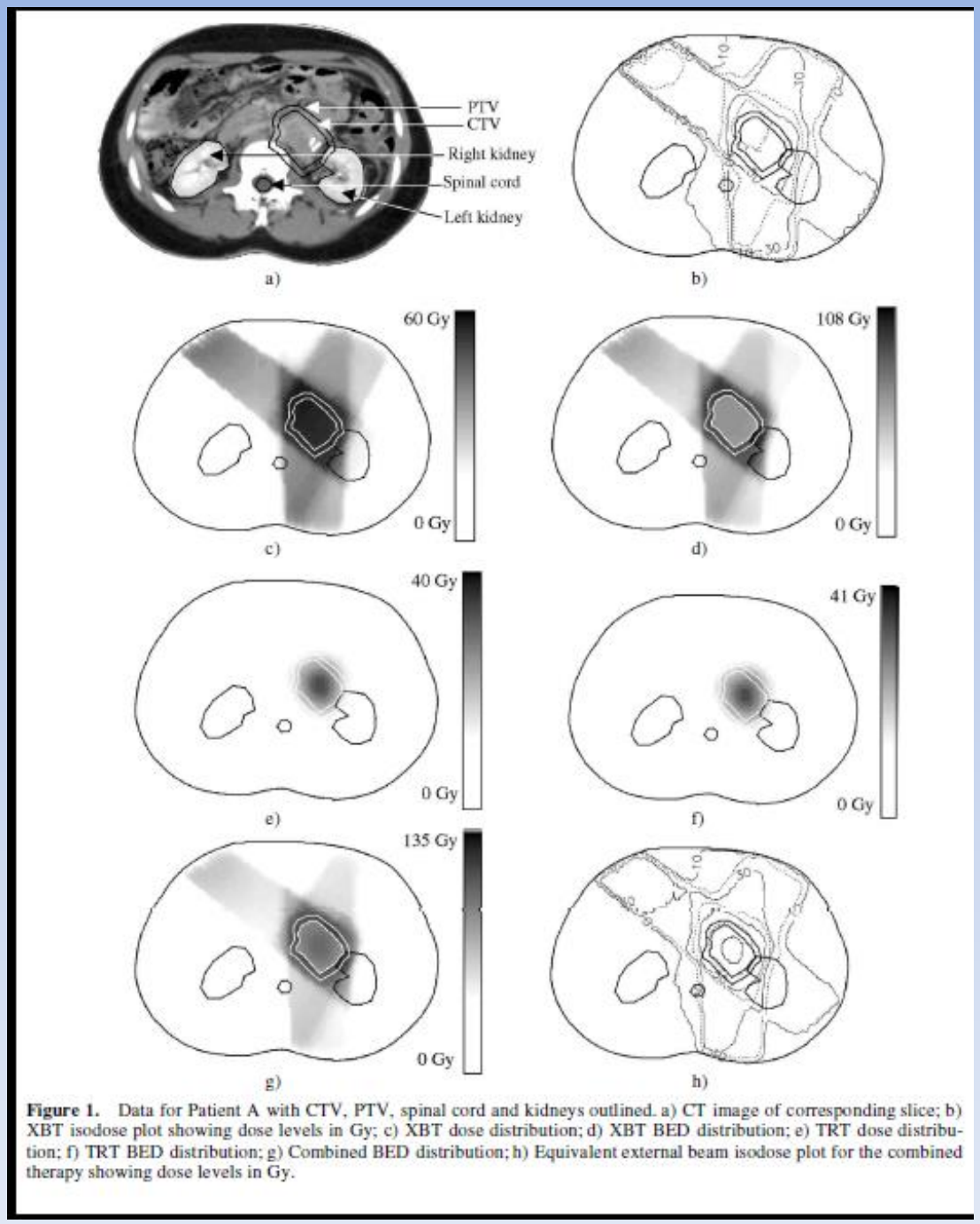

Figure 1. Data for Patient A with CTV, PTV, spinal cord and kidneys outlined. a) CT image of corresponding slice; b) XBT isodose plot showing dose levels in Gy; c) XBT dose distribution; d) XBT BED distribution; e) TRT dose distribution; f) TRT BED distribution; g) Combined BED distribution; h) Equivalent external beam isodose plot for the combined therapy showing dose levels in Gy.

Bodey et al. 2003

STRATOS Dosimetry Solution is an advanced research software package for 3-dimensional dose calculation in nuclear medicine, allowing you to calculate and visualize patient-specific dose maps for targeted therapeutic radionuclide agents based on antibodies or peptides. STRATOS Dosimetry Solution optimally supports research focussed on image-based dosimetry using SPECT/CT and PET/CT data.

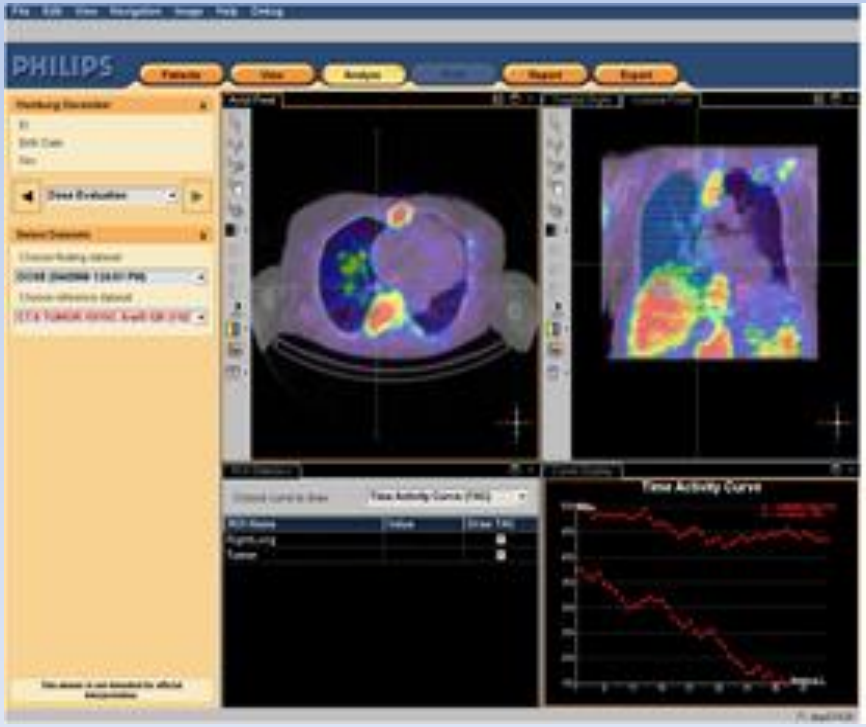

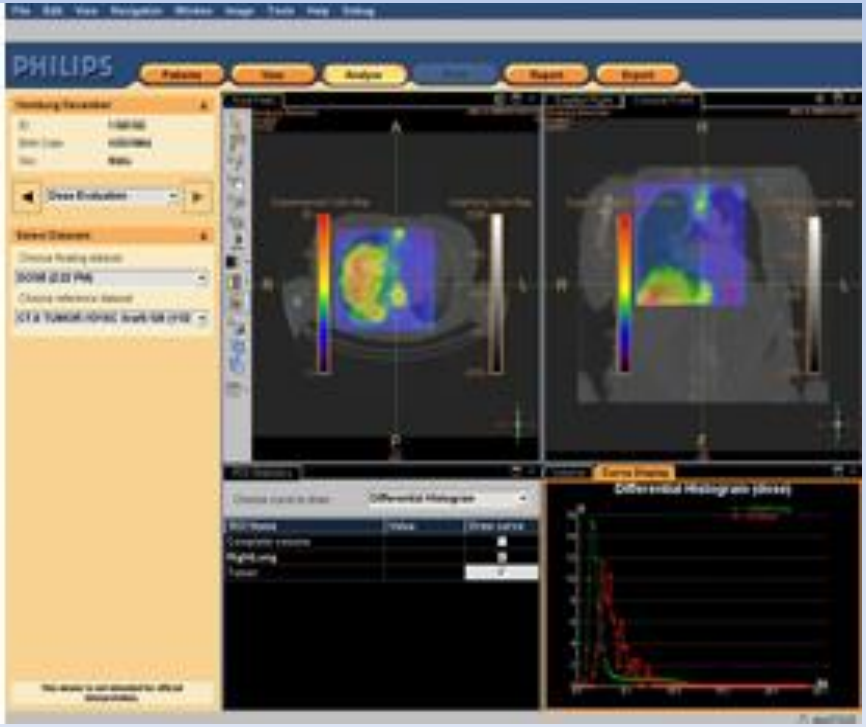

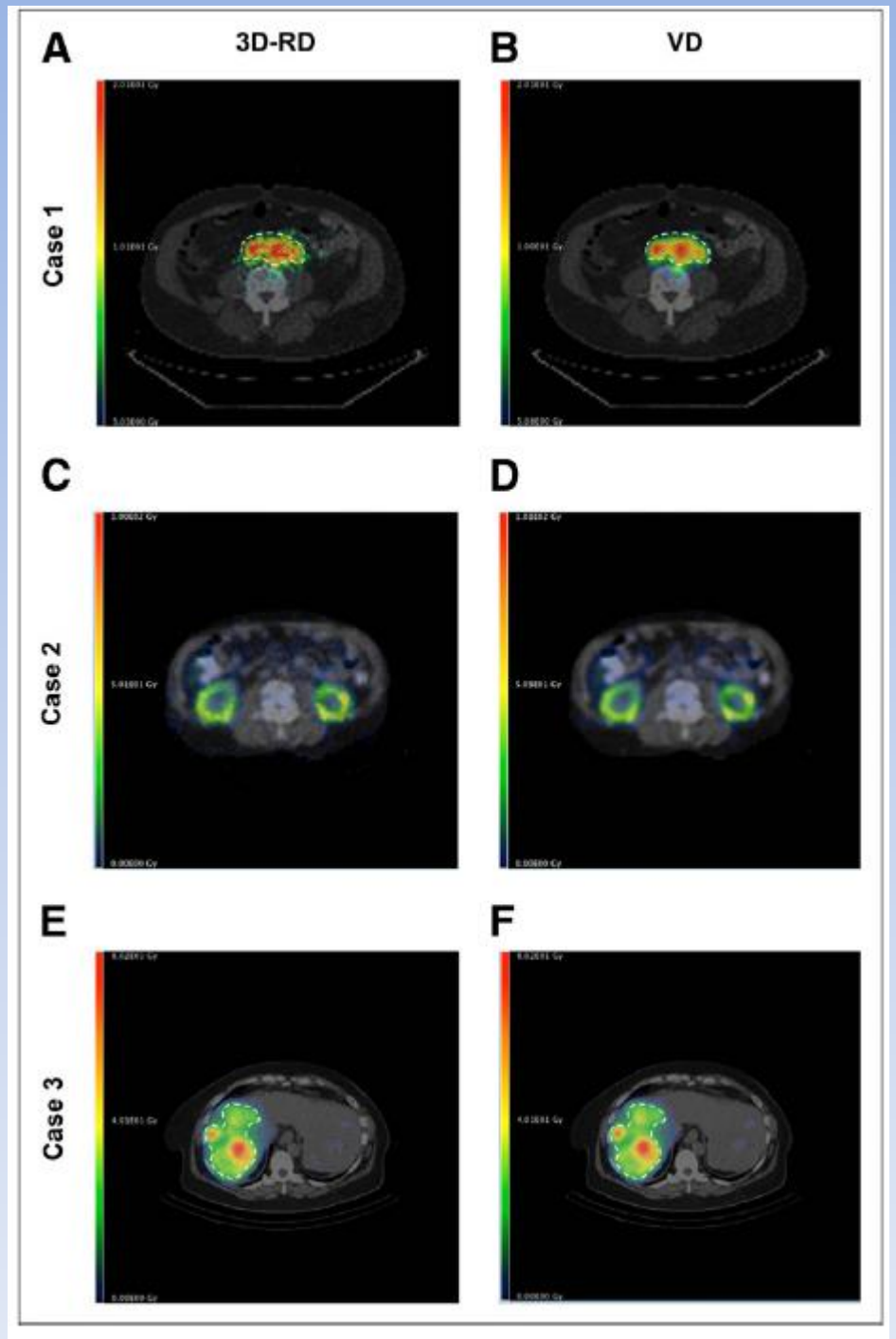

Dieudonne J Nucl Med 2013;
54:236–243

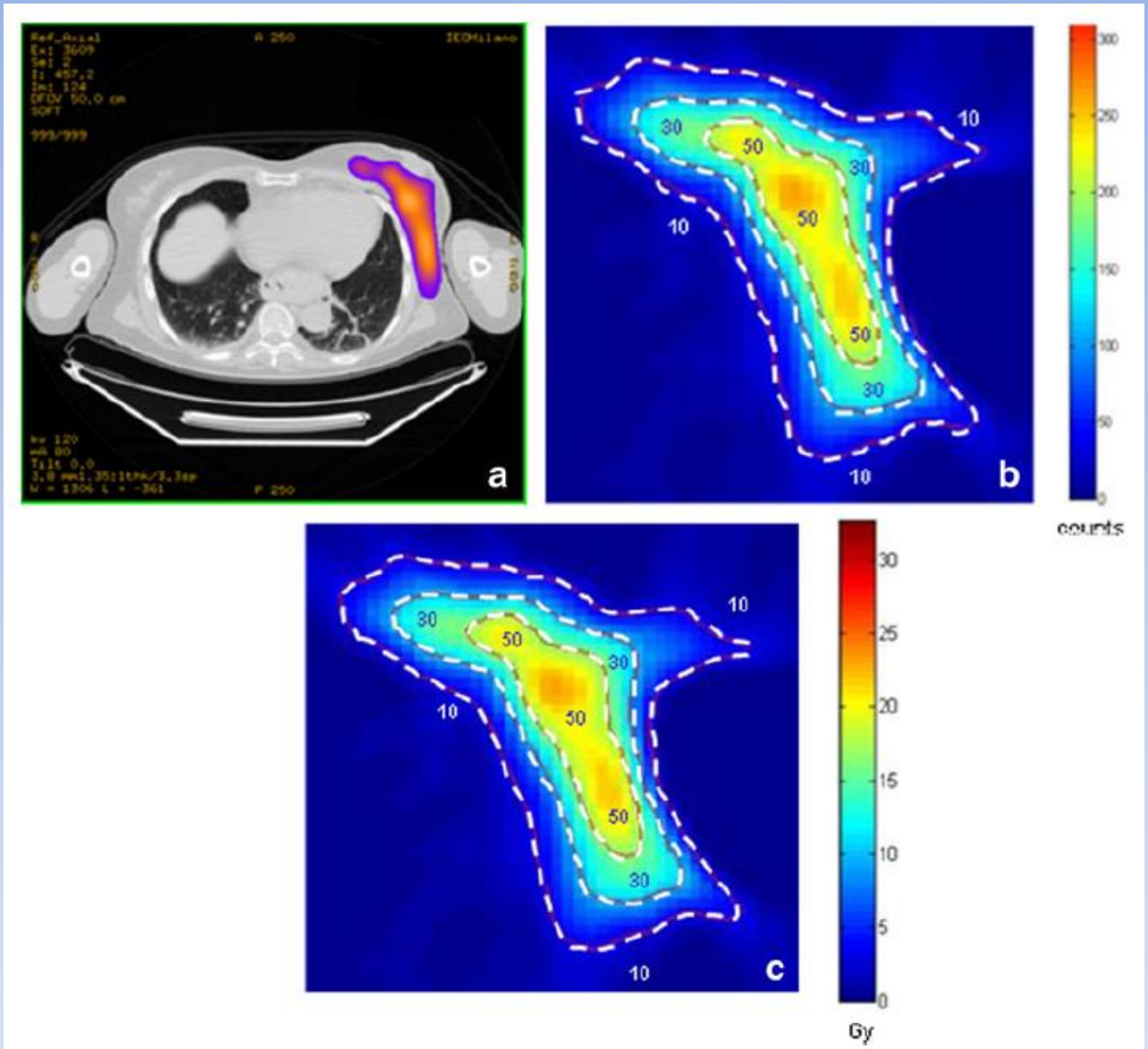

Ferrari et al. Eur J Nucl Med Mol Imaging (2012) 39:1702–1711

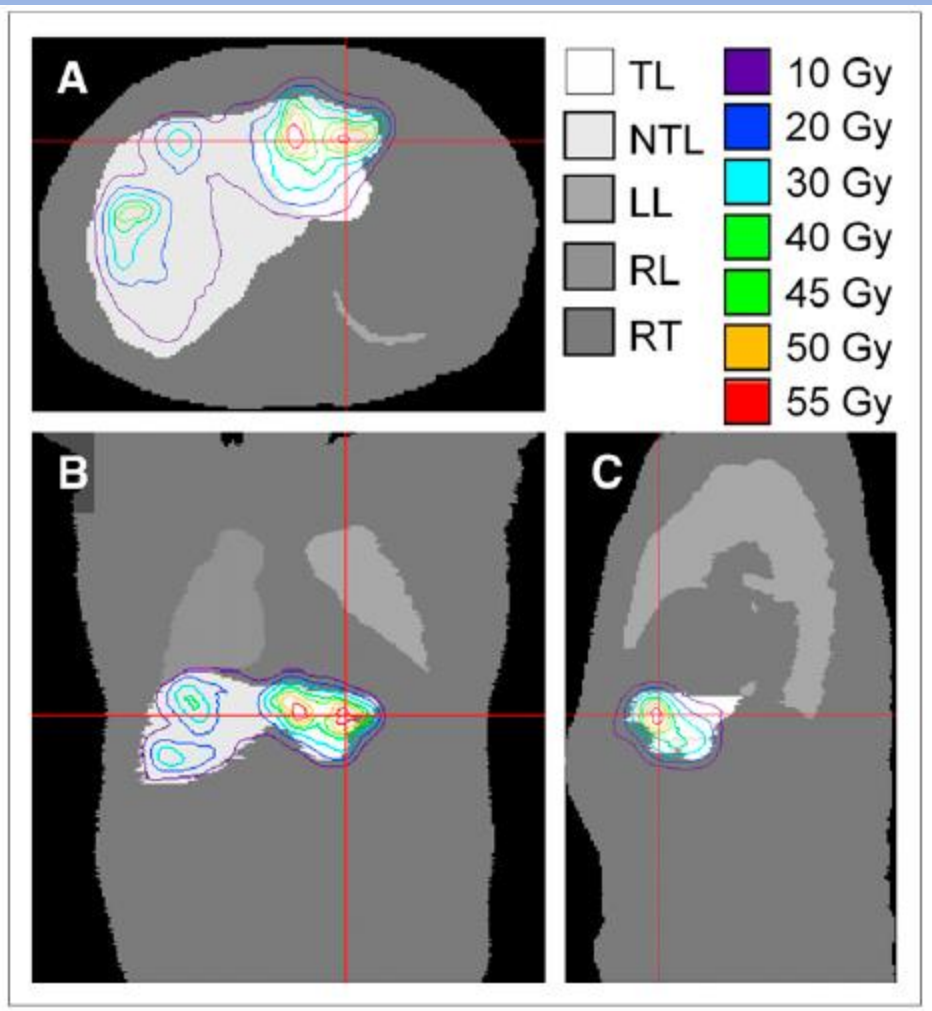

FIGURE 2. Axial (A), coronal (B), and sagittal (C) views of isodose curves superimposed on patient-specific voxel phantom obtained for evaluation E3 with an injected activity of 1 GBq. LL = left lung; RL = right lung.

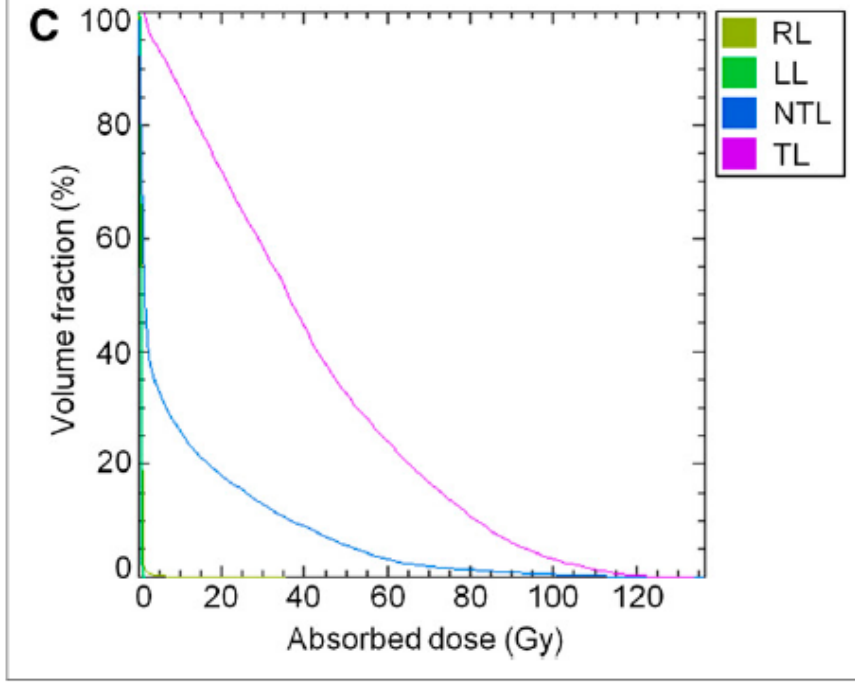

FIGURE 3. DVHs for RL, LL, NTL, and TL obtained for evaluation E3 (A), E10 (B), and E11 (C) with an injected activity of 1 GBq. LL = left lung; RL = right lung.

Petitguillaume et al. JNM 2014; 55:405-413

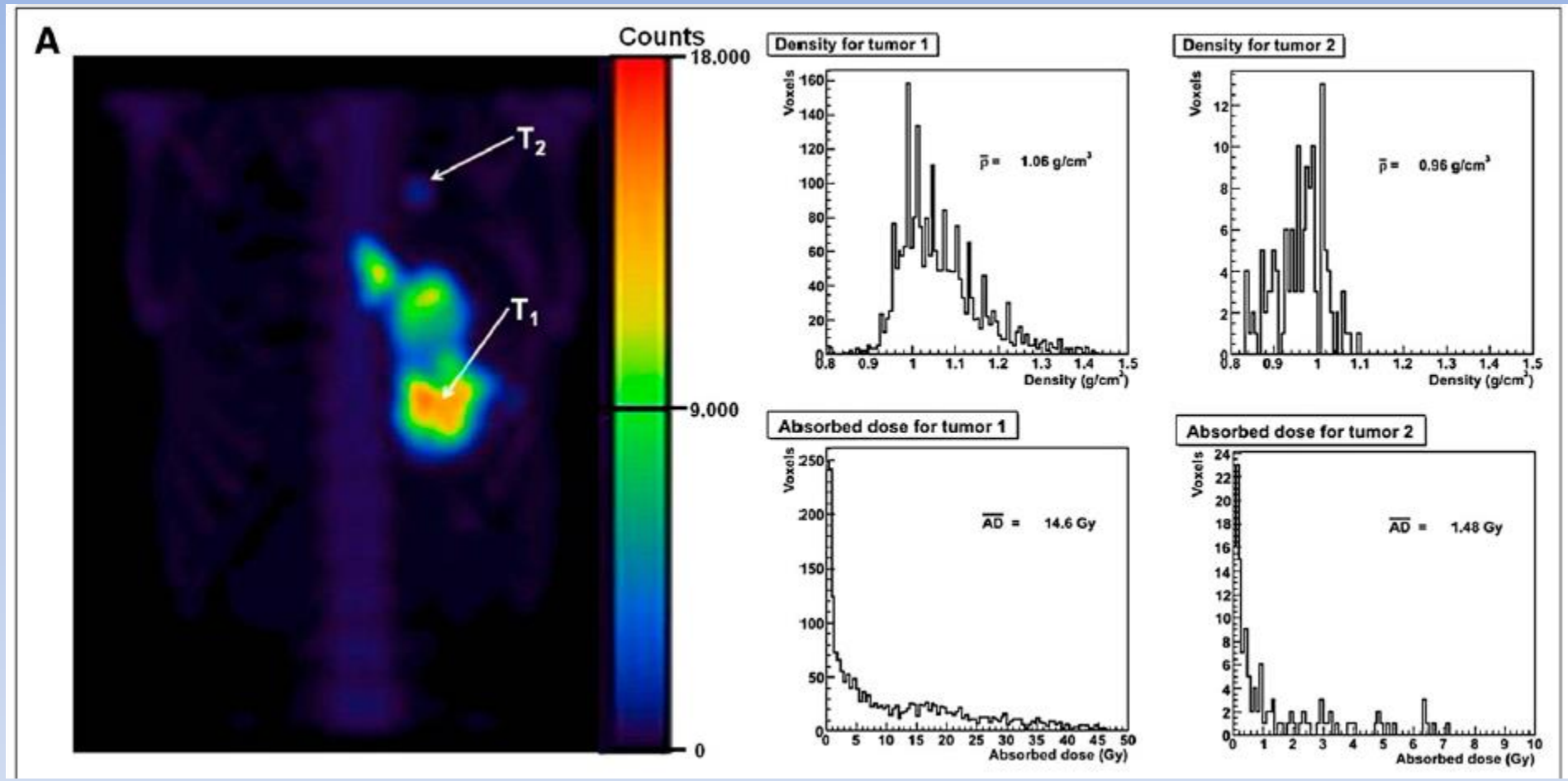

Senthamizhchelvan et al. JNM 2012; 53:215-224

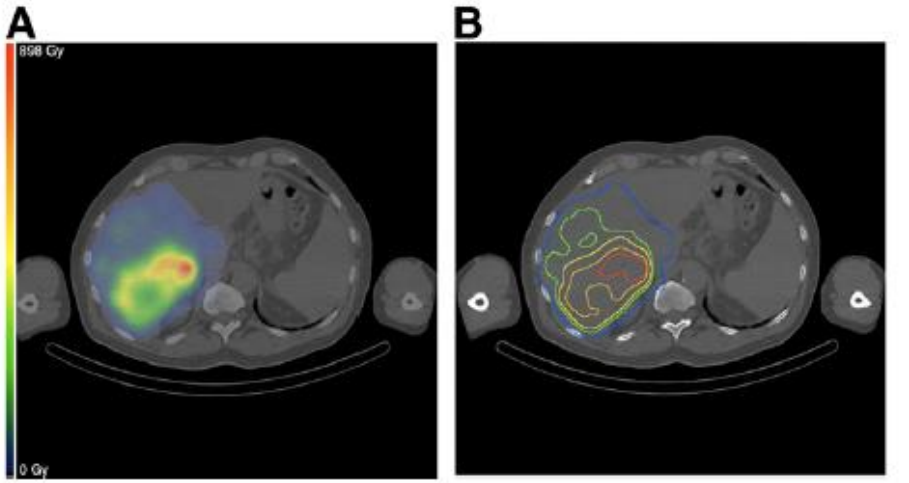

FIGURE 2. 3D dosimetry results for patient 1. (A) Transverse slice of 3D dose map fused with CT. (B) Isodose curves superimposed on transverse slice of CT. Blue curve = isodose 1% of maximum dose; green curve = isodose 5% of maximum dose; yellow curve = isodose 10% of maximum dose; orange curve = isodose 30% of maximum dose; red curve = isodose 50% of maximum dose.

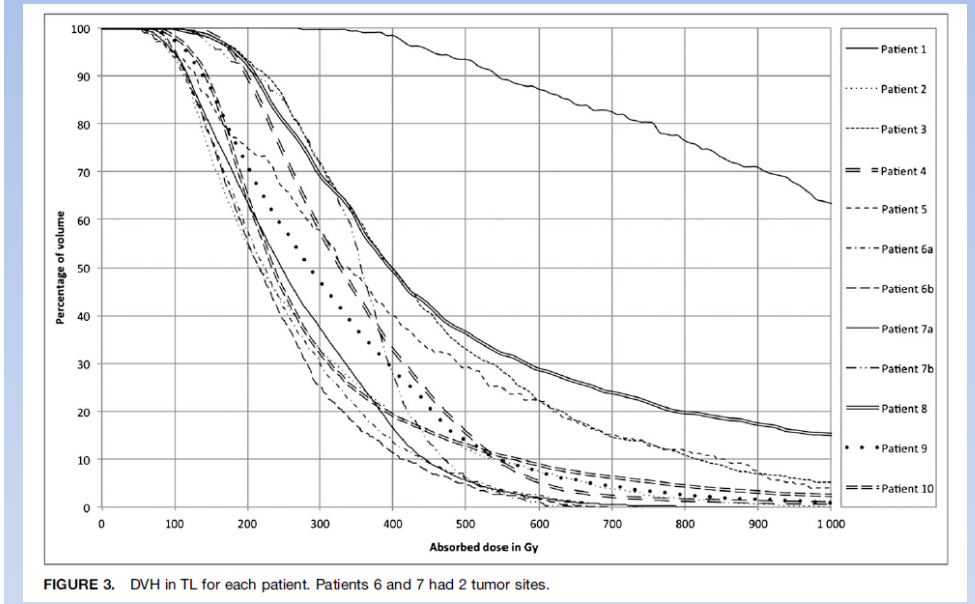

FIGURE 3. DVH in TL for each patient. Patients 6 and 7 had 2 tumor sites.

Dieudonne et al. JNM 2011:52:1930-1937

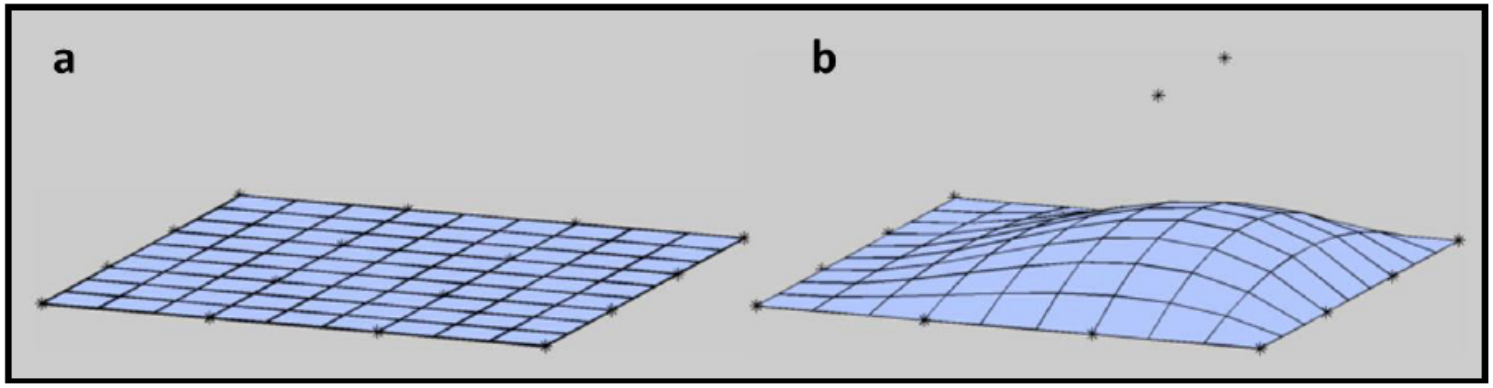

Figure IV.2: Modification of NURBS surface by moving control points. (a) NURBS representation of a plane with controls points (*) aligned on the surface. (b) Surface with shaped altered by translating two of the center control points in the z-axis.

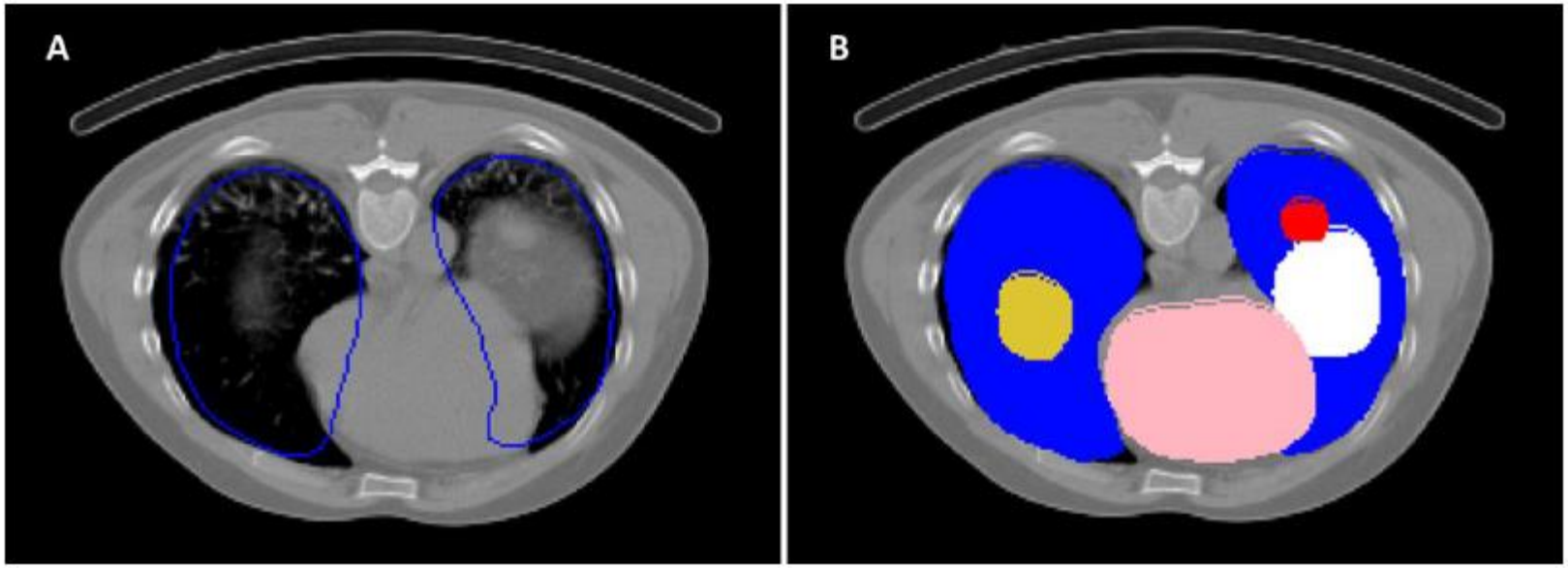

Figure IV.11: Overlap of lungs at base before deforming structures to match patient (a) and after modification (b). The white area is the left diaphragm that is voxelized as body and replaced by other organs including spleen (red), stomach and heart (pink).

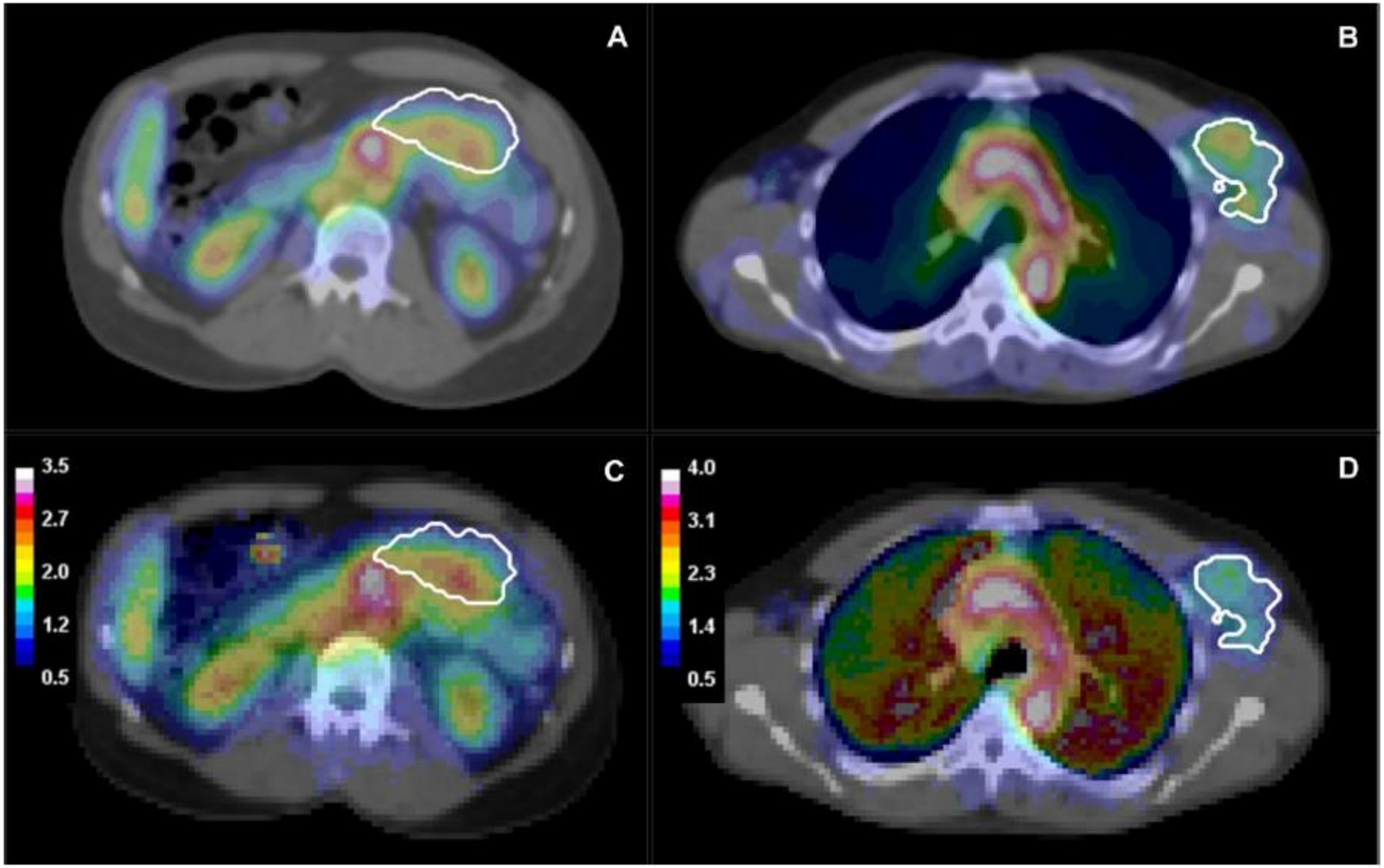

Figure V.1: Fused SPECT/CT images for (a) Patient 1 and (b) Patient 2 with matching 3D dose maps overlaid on CT for (c) Patient 1 and (d) Patient 2. The dose maps are displayed in units of Gy.

Do Calculated Doses Predict Biological Effects?

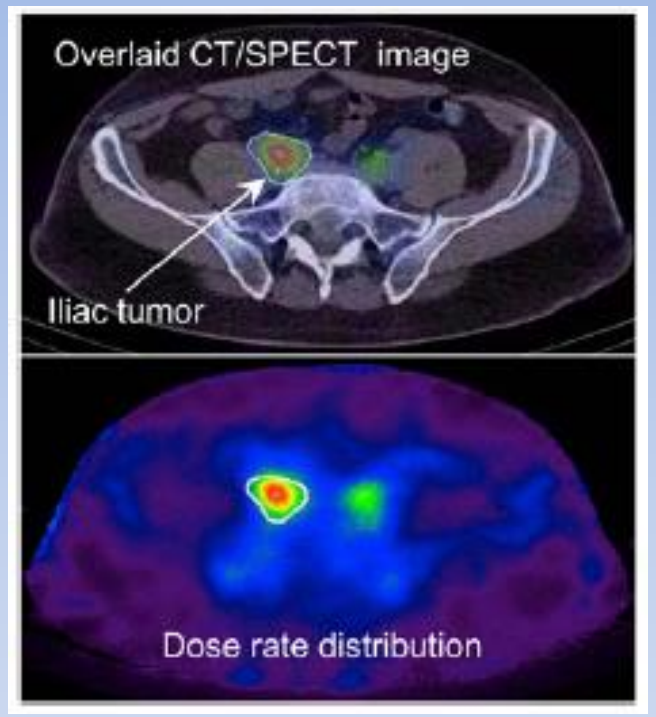

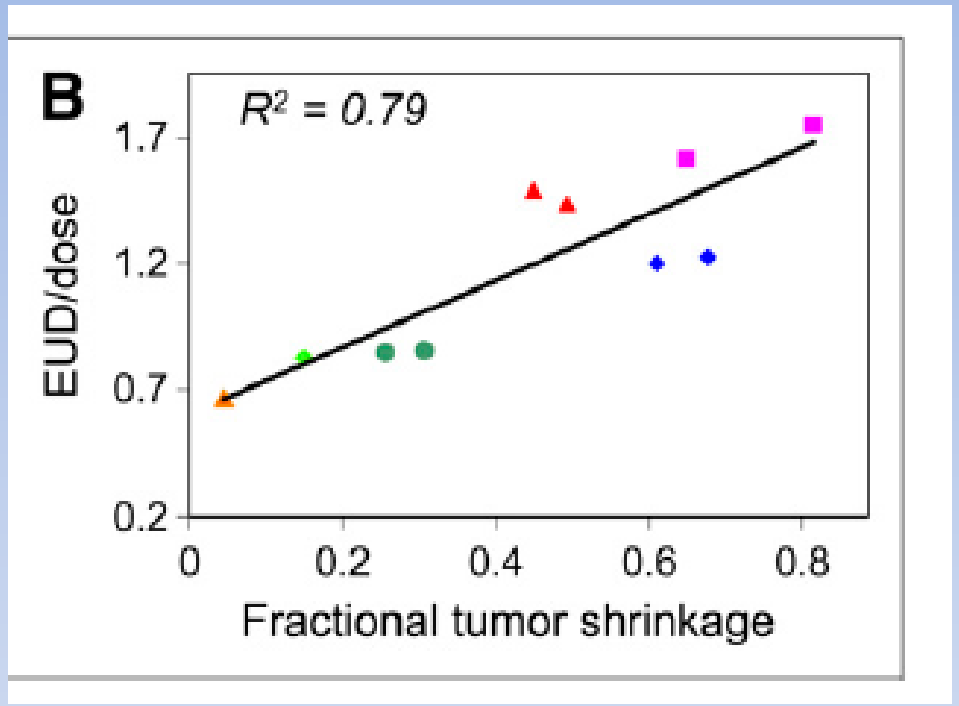

Amro et al. J Nucl Med 2010; 51:654–659

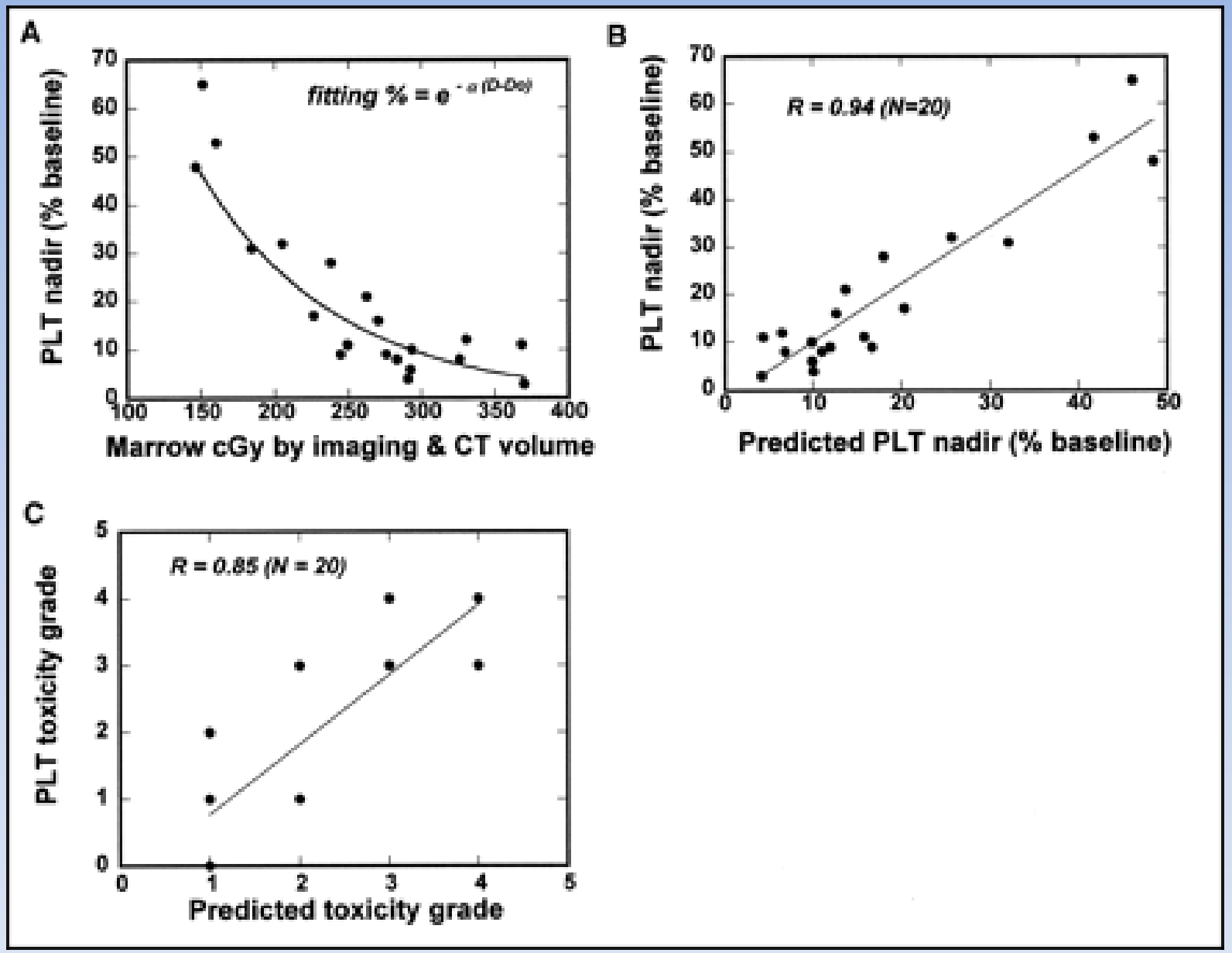

Shen et al. JNM 43 No. 9 1245-1253, 2002

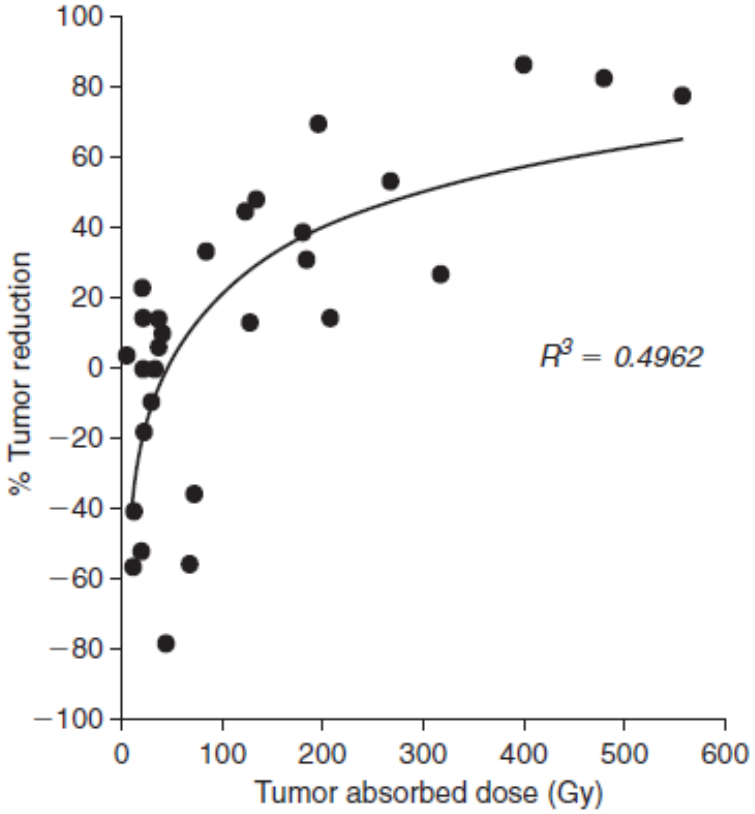

Figure 6. Tumor dose-response characterized by Pauwels et al.[48] with ^{90}Y-DOTATOC. Reprinted with permission of the Society of Nuclear Medicine.

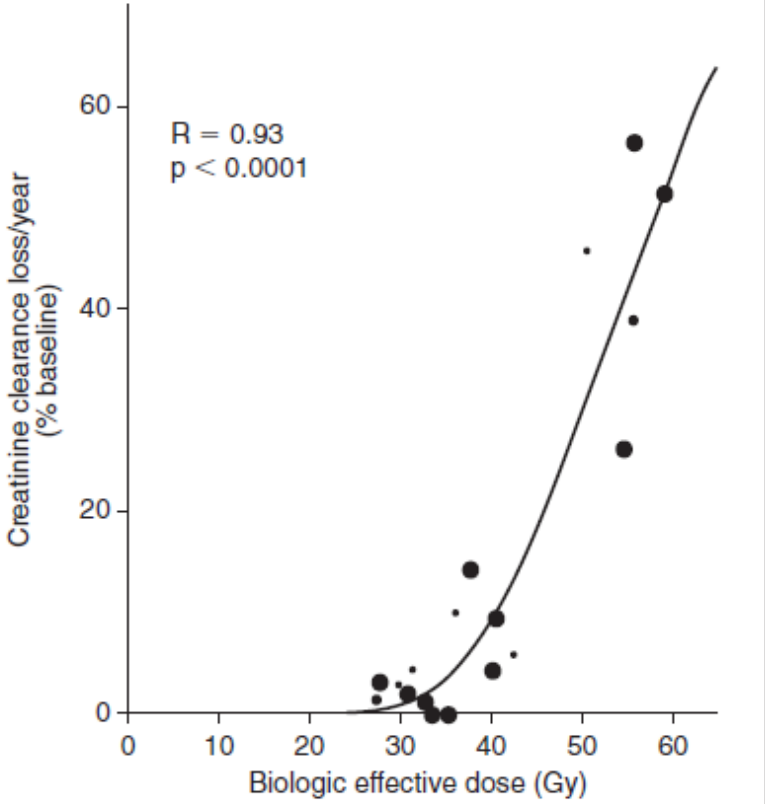

Figure 7. Plot from Barone et al.[51] showing prediction of kidney toxicity from patient-individualized dose calculations in the use of ^{90}Y (DOTATOC). (Larger and smaller dots on the plot were used to indicate the number of treatment cycles received by different patients.) Reprinted with permission of the Society of Nuclear Medicine.

Dose rates and renal toxicity

TABLE 2
Comparisons of Absorbed Doses and Dose Rates to Kidneys with Radionuclide Therapies

Therapy	N_{frac}	A (GBq)	D (Gy)	R_0 (Gy/h)	RE	BED (Gy)
^{90}Y-DOTA-octreotide	3	13.3	27	0.15	1.2	32
^{111}In-DTPA-octreotide	8	83	34	0.07	1.1	37
^{177}Lu-DOTA-octreotate	4	29.6	26	0.04	1.1	29
^{166}Ho-DOTMP	1	167	7.5–15	4.2–8.4	2.4–3.7	18.0–55.5
External-beam irradiation	16	NA	23	NA	1.6	37
Total-body irradiation	6	NA	12	NA	1.8	22

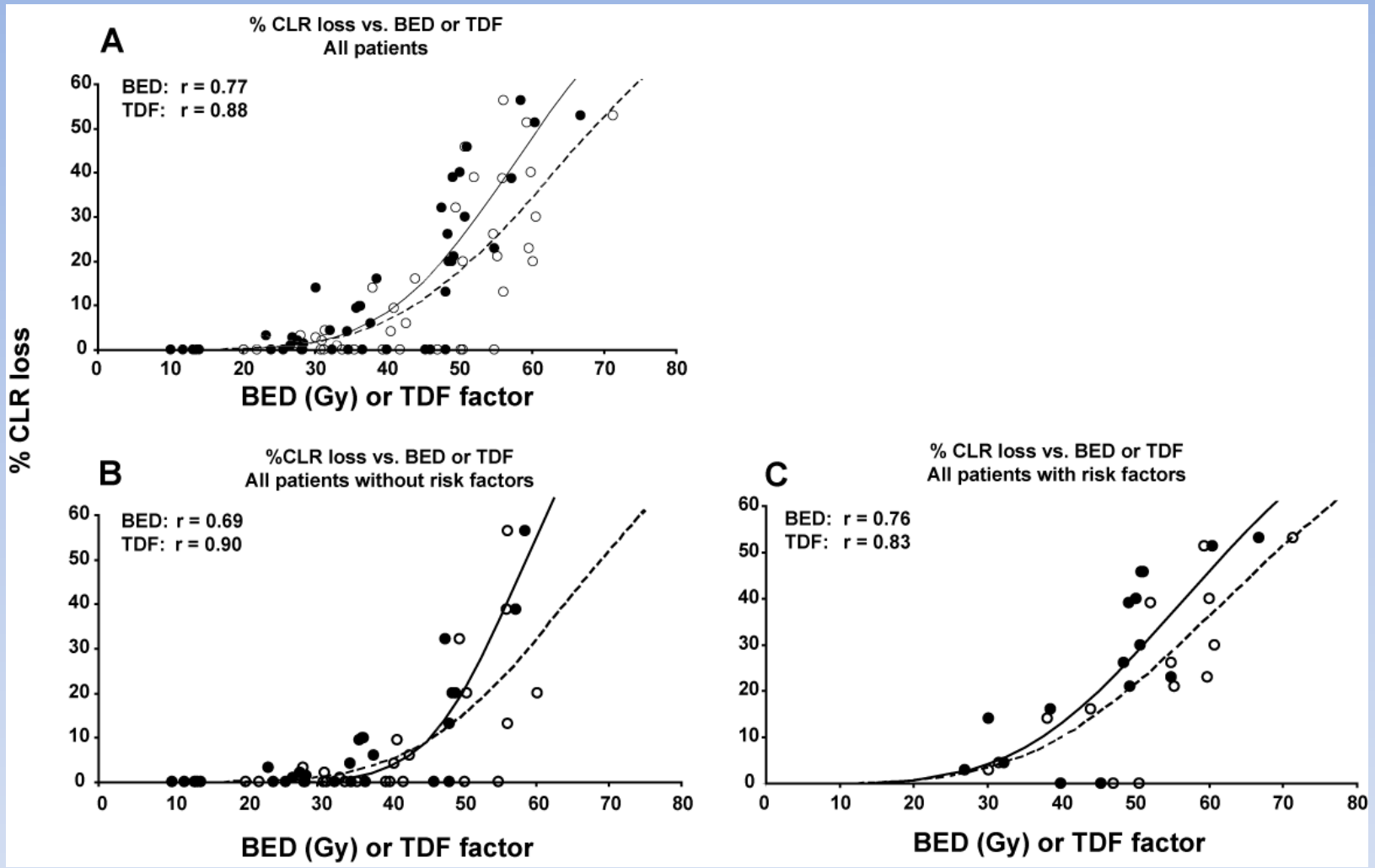

% CLR loss versus BED (open circles/dashed line) or TDF (solid circles/solid line) for the combined Barone and Bodei data sets. (A) All patients. (B) All patients without risk factors. (C) All patients with risk factors.

PFS Stratified by Tumor Dose

- Longer PFS for mean tumor absorbed dose >200 cGy
- Median PFS
  - 13.6 mo (>200 cGy)
  - 1.9 mo (<200 cGy)

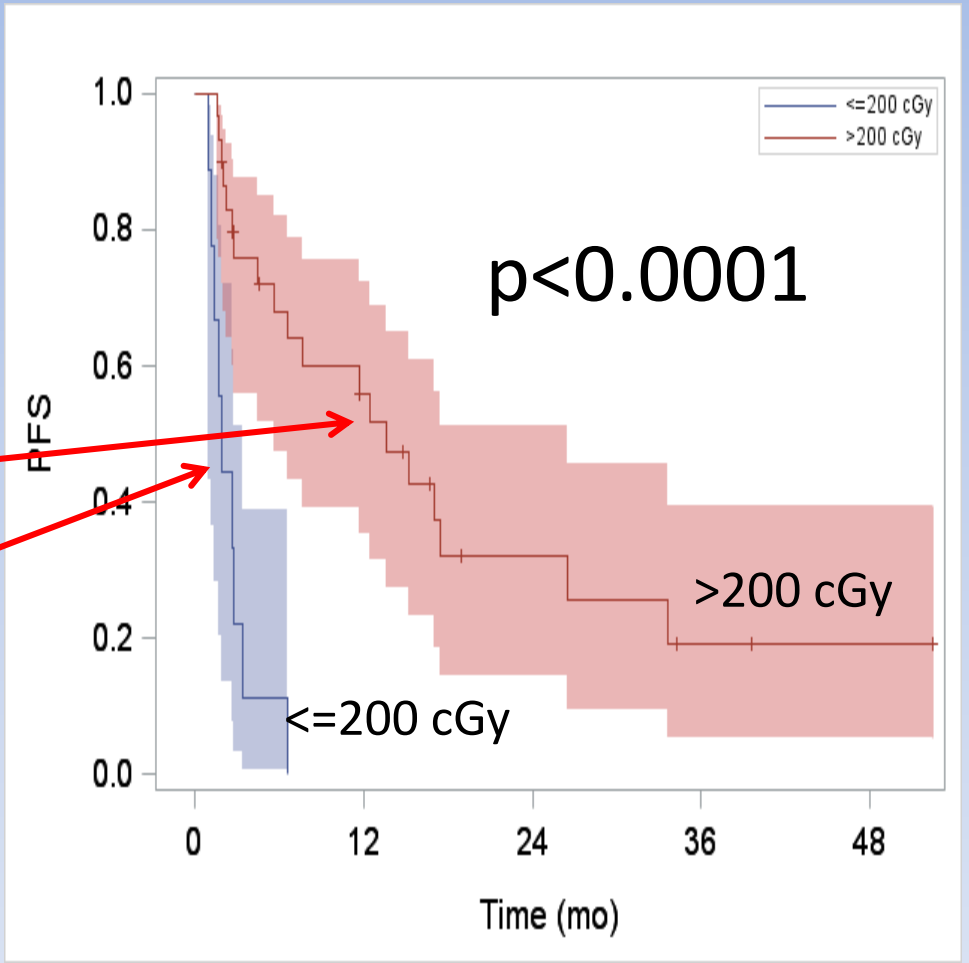

Philosophical Point

- When is a Gy a Gy? Almost never!
- 1 Gy of gamma whole body…
- 1 Gy of alpha?
- 1 Gy of beta or gamma in therapy?

$$BED = D\left(1 + \frac{d}{\alpha/\beta}\right)$$

$$mEUD = \frac{\left(\sum_{i=1}^{N} v_i \cdot BED_i^a\right)^{1/a}}{C}$$

- Medium transfer bystander effects? Dose is zero!
- 0 ⊗ anything = 0

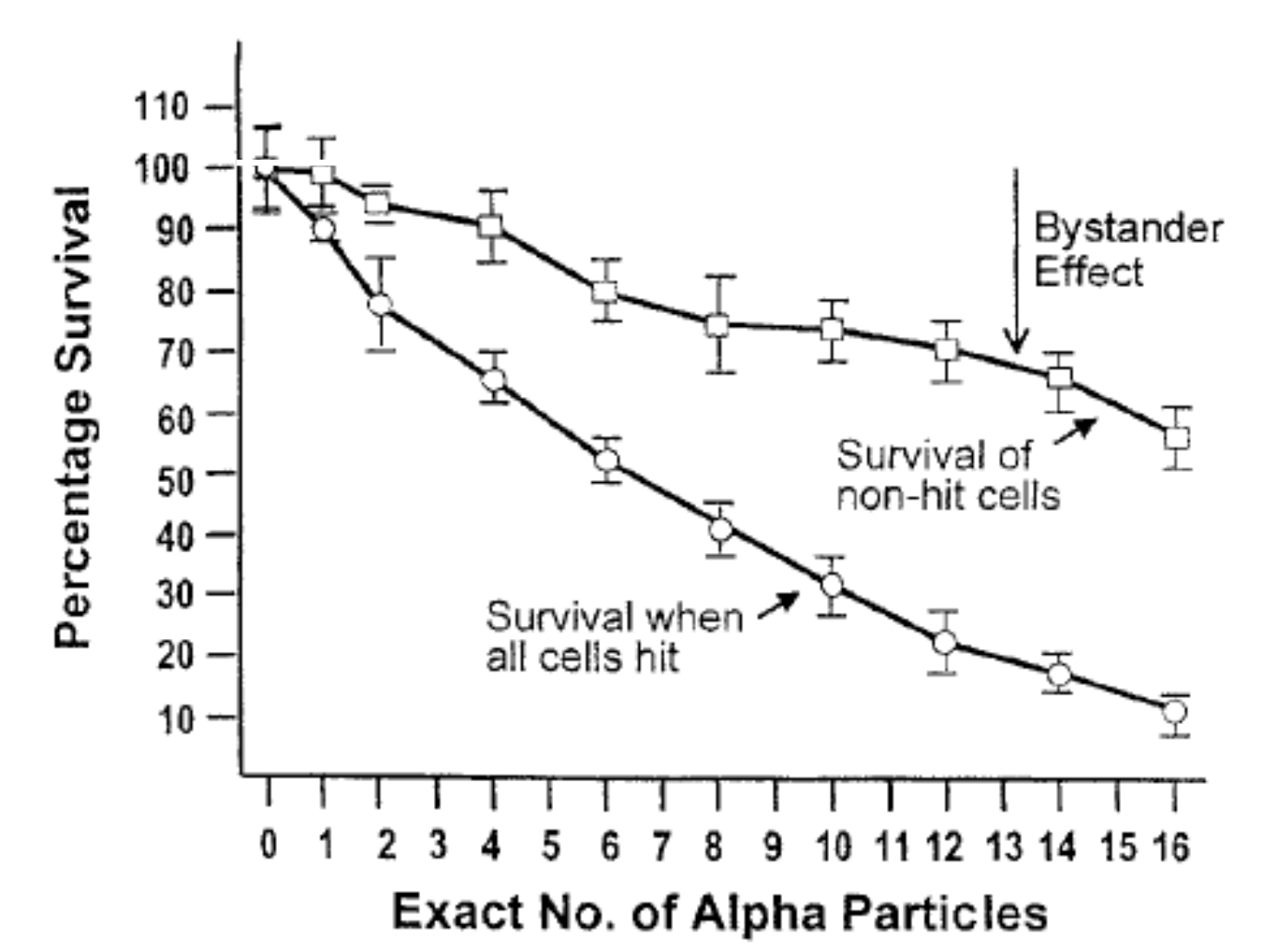

Bystander effect shown by Hall[20] in V79 cells in which all cells or 10% of cells were struck by 1-16 alpha particles.

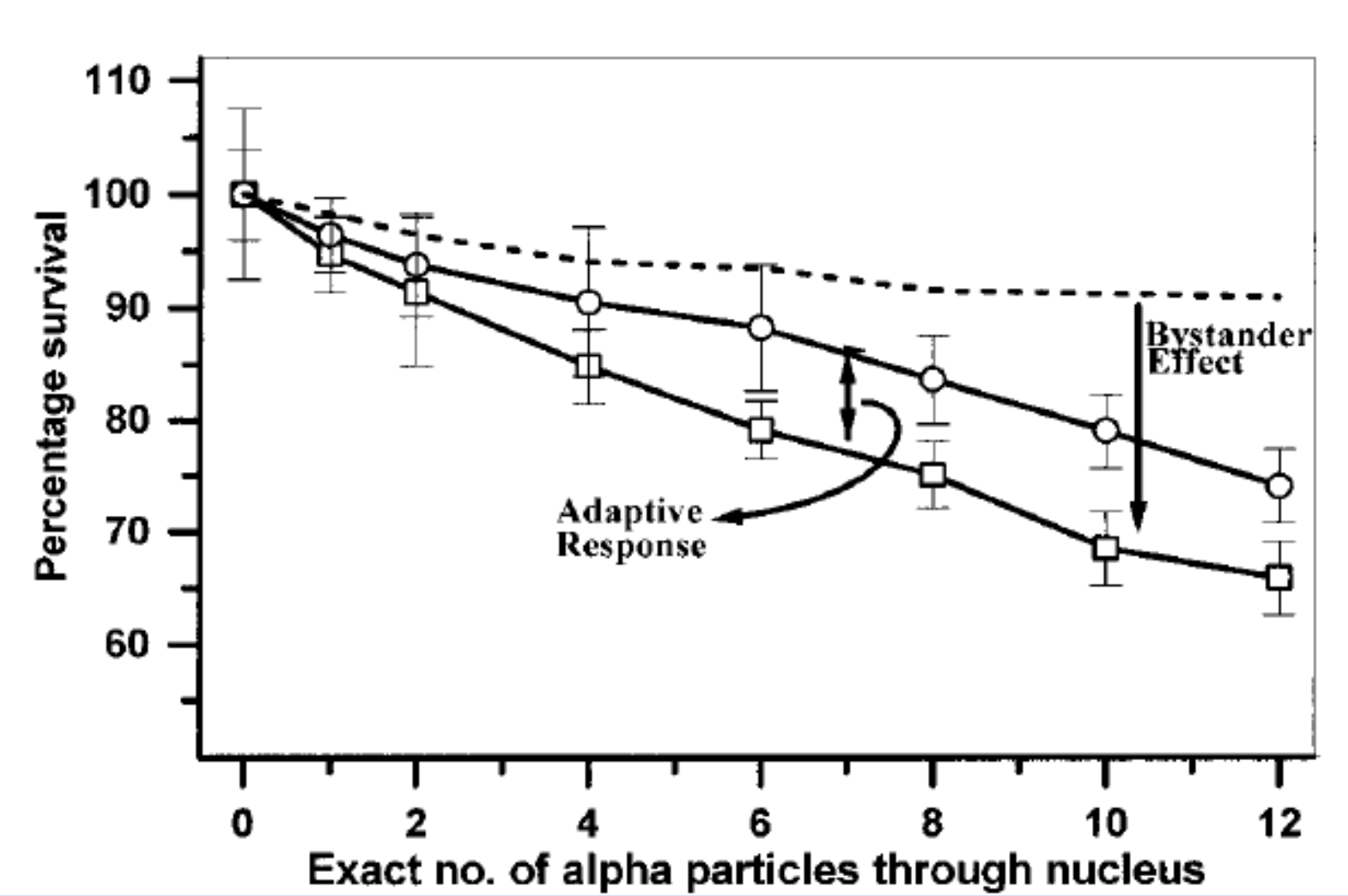

Sawant et al. Radiation Research, 156, 177–180 (2001)

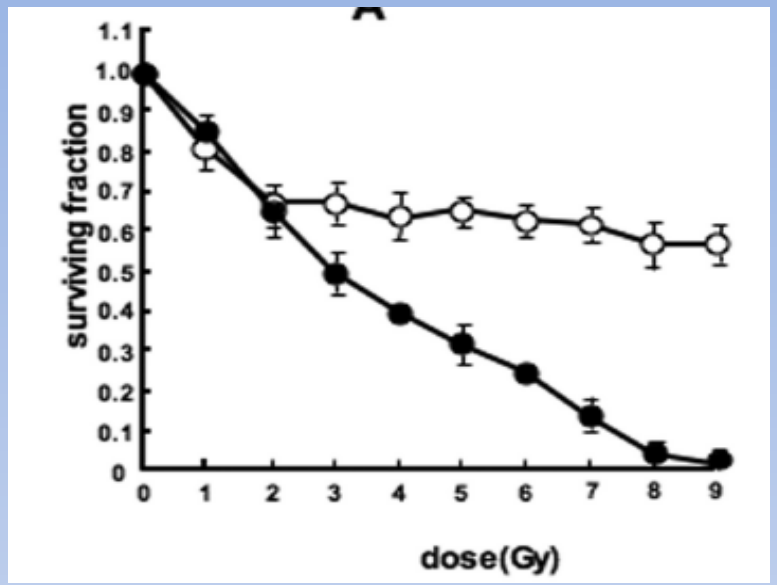

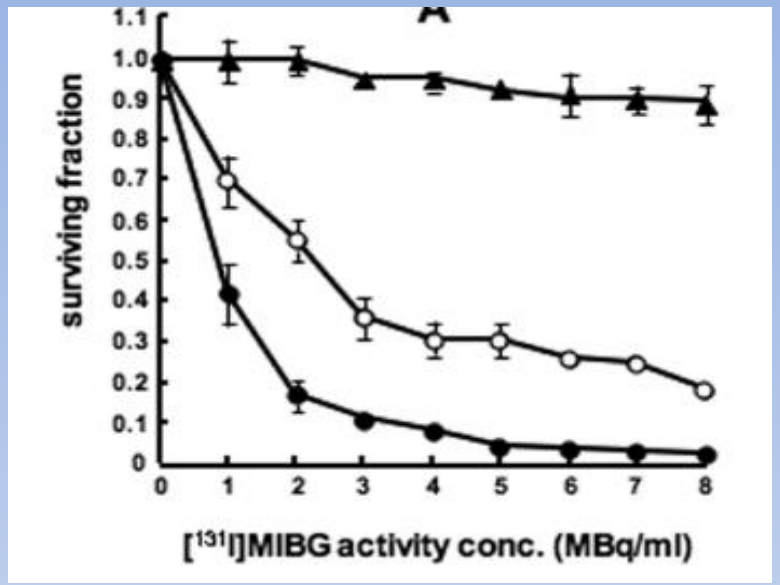

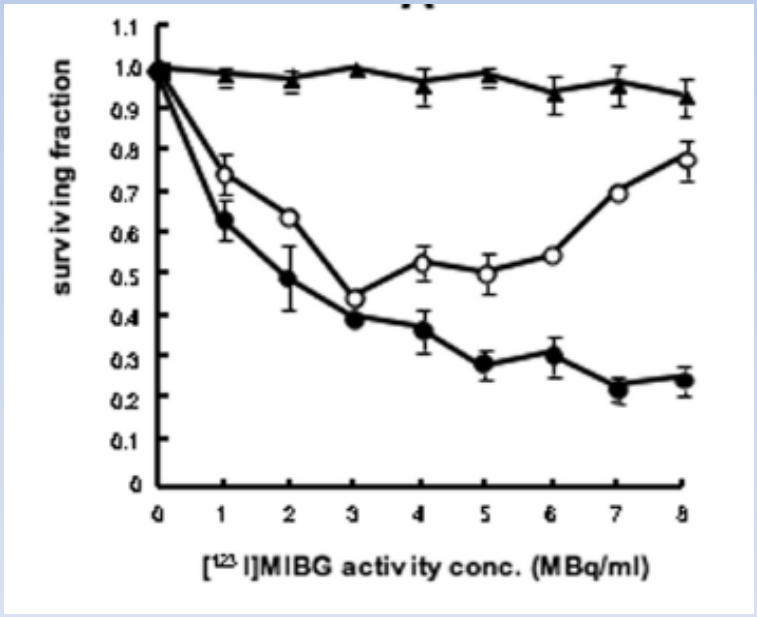

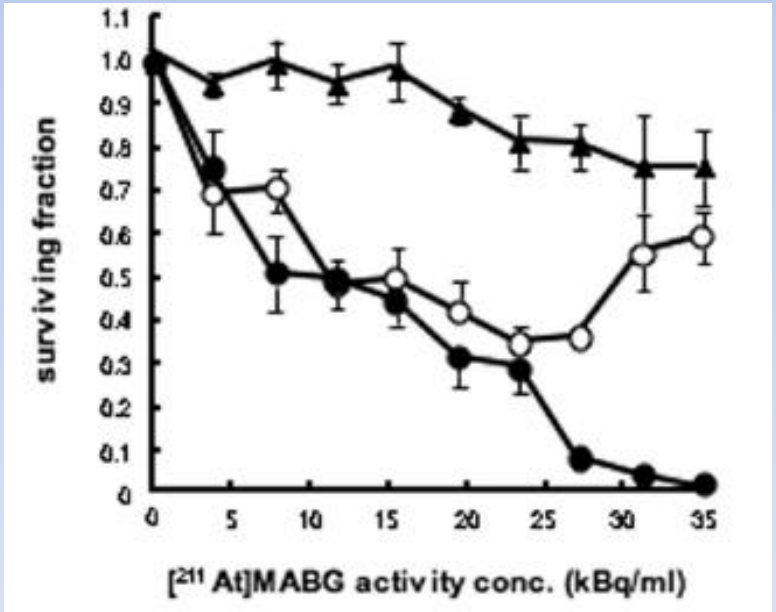

Mairs RJ, Fullerton NE, Zalutsky MR, Boyd M. Targeted radiotherapy: microgray doses and the bystander effect. Dose-Response, 5:204–213, 2007.

In Vivo Bystander Effects: ^{123}IUdR and ^{125}IUdR

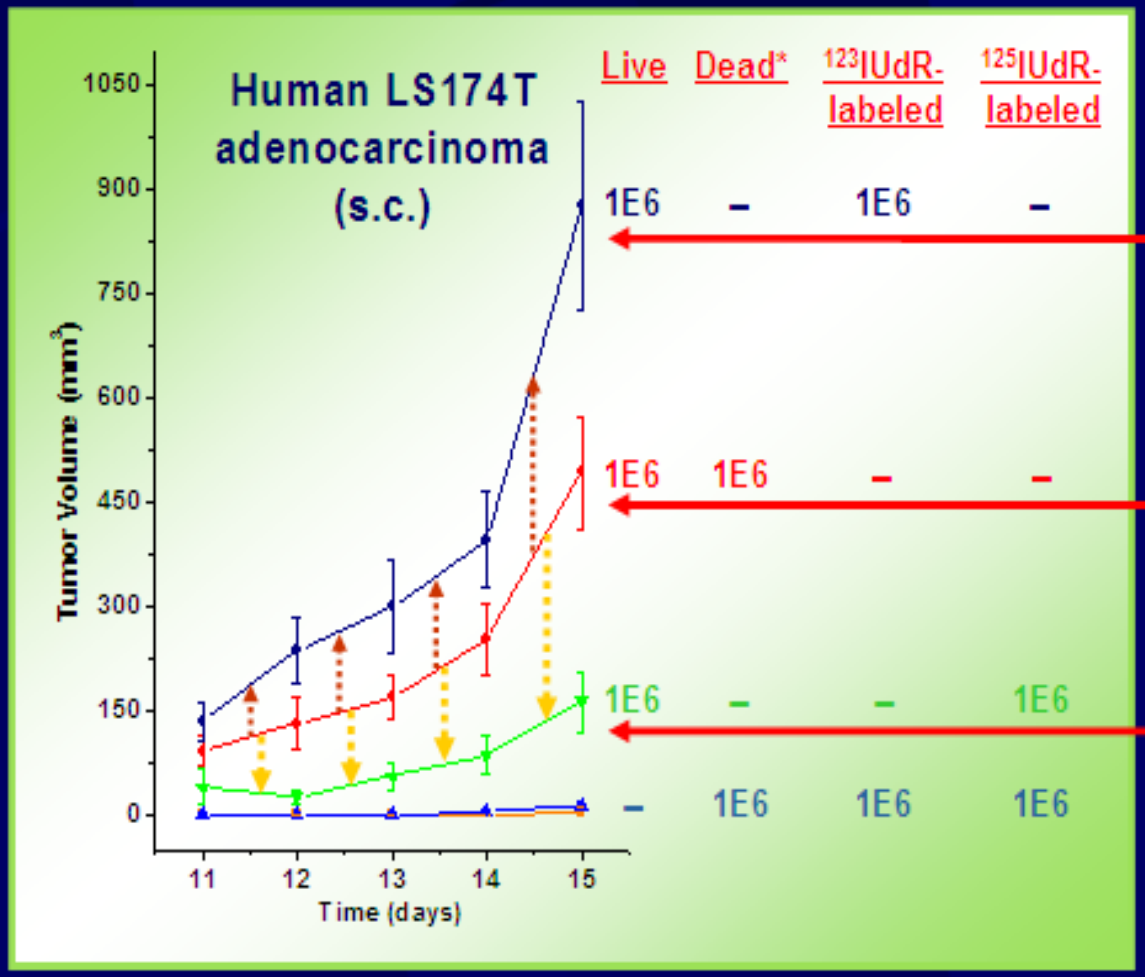

* Freeze–defrost 3 times

Conlusions

- Whole organ dosimetry methods are well standardized.
- With mass adjustment, this may suffice for some applications.
- 3D dosimetry methods have been demonstrated by many centers. Quantitative SPECT and PET have good accuracy when done correctly.
- Our understanding of dosimetric quantities is undergoing change. Collaboration is vital.